

# VARIABLE COSMOLOGICAL CONSTANT - GEOMETRY AND PHYSICS

Irina Dymnikova

*Institute of Mathematics, Informatics and Physics,  
University of Warmia and Mazury in Olsztyn, 10-561 Olsztyn, Poland*

**The talk at the International Seminar "Mathematical Physics and Applied Mathematics" in memory of Professor Georgij Abramovich Grinberg (1900-1991), 16 June 2000, St-Petersburg, Russia.**

## DEDICATION

*The results presented here probably would have never been obtained without unforgettable hours spent by author, throughout twenty years 1968-1988, in conversations with people from the Mathematical Physics Department of the A.F. Ioffe Institute in Leningrad. It was oasis of deep respect for human being and products of his thinking. People of this Department created atmosphere in which one immediately got a feeling that not only he is able to produce something but this is just his natural state. Coming there I, for one, felt like a fish moved from a pan into a water. I thank the Providence for this gift and dedicate this paper to the blessed memory of Georgij Abramovich Grinberg, Nikolaj Nikolajevich Lebedev and Jakov Solomonovich Ufland.*

## Abstract

We describe the dynamics of a cosmological term in the spherically symmetric case by an  $r$ -dependent second rank symmetric tensor  $\Lambda_{\mu\nu}$  invariant under boosts in the radial direction. The cosmological tensor  $\Lambda_{\mu\nu}$  represents the extension of the Einstein cosmological term  $\Lambda g_{\mu\nu}$  which allows it to be variable. This possibility is based on the Petrov classification scheme and Einstein field equations in the spherically symmetric case. The inflationary equation of state  $p = -\rho$  is satisfied by the radial pressure,  $p_r^\Lambda = -\rho^\Lambda$ . The tangential pressure  $p_\perp^\Lambda$  is calculated from the conservation equation  $\Lambda_{\nu;\mu}^\mu = 0$ . The solutions of Einstein equations with cosmological term  $\Lambda_{\mu\nu}$  describe several types of globally regular self-gravitating vacuum configurations including vacuum nonsingular black holes. In this case global structure of space-time contains an infinite set of black and white holes, whose past and future singularities are replaced with the value of cosmological constant  $\Lambda$  of the scale of symmetry restoration, at the background of asymptotically flat or asymptotically de Sitter (with  $\lambda < \Lambda$ ) universes. Geodesics structure of space-time demonstrates possibility of travelling into other universes through the interior of a  $\Lambda$  black hole. In the course of Hawking evaporation of a  $\Lambda$ BH, a second-order phase transition occurs, and globally regular configuration evolves towards a self-gravitating particlelike structure ( $\Lambda$  particle) at the background of Minkowski or de Sitter space.

PACS numbers: 04.70.Bw, 04.20.Dw

## I. INTRODUCTION

The cosmological constant was introduced by Einstein in 1917 as the universal repulsion to make the Universe static in accordance with generally accepted picture of that time. The Einstein equations with a cosmological term read

$$G_{\mu\nu} + \Lambda g_{\mu\nu} = -\kappa T_{\mu\nu} \quad (1)$$

where  $G_{\mu\nu}$  is the Einstein tensor,  $g_{\mu\nu}$  is the metric,  $T_{\mu\nu}$  is the stress-energy tensor of a matter,  $\kappa$  is the Einstein gravitational constant related to the Newton gravitational constant  $G$  by  $\kappa = 8\pi G c^{-4}$ , and  $\Lambda$  is the cosmological constant. In the absence of matter described by  $T_{\mu\nu}$ ,  $\Lambda$  must be constant, since the Bianchi identities guarantee vanishing covariant divergence of the Einstein tensor,  $G^{\mu\nu}_{;\nu} = 0$ , while  $g^{\mu\nu}_{;\nu} = 0$  by definition.

In 1922 Friedmann found nonstationary solutions to the Einstein equations (1) describing an expanding universe, and in 1926-1929 the Hubble observations established the fact that our Universe is expanding.

At the late 40-s cosmological constant was called for second time to make the Universe stationary. In steady-state Bondi-Gold-Hoyle cosmology [10,42] permanent creation of matter has been assumed, with cosmological constant related to  $C$ -field responsible for this process.

Third coming of cosmological constant in the 70-s was quite spectacular. It was called for to make the very early Universe blowing up. The main reason came from the problem of initial conditions for an expanding Universe. A closed Universe starting from initial Planckian density  $\rho_{Pl} \sim 10^{94} g\ cm^{-3}$  and evolving in accordance with the standard FRW cosmology, would recollapse back in Planckian time  $t_{age} \sim 10^{-43} s$ . For open or spatially flat Universe we would have today density  $\rho < 10^{-90} g\ cm^{-3}$ . Looking back we would have to conclude that observable Universe would expand from a region of  $a(t_{Pl}) \sim 10^{-13} cm$  that contained a huge number of causally disconnected regions of Planckian size, which makes impossible to explain presently observed homo-

geneity and isotropy of the Universe (for review see [43]).

Analyzing in 1930 the problem of the Universe evolution Sir A. Eddington made two remarks [29]. First concerned the problem of initial conditions: "Difficulty in admitting this situation is that it seems to require some sudden and incomprehensible origin of all things". Second concerned the de Sitter solution. In the case of absence of a matter described by  $T_{\mu\nu}$ , the solution to the Einstein equation (1), found by de Sitter in 1917, is de Sitter geometry with constant positive curvature  $R = 4\Lambda$

$$ds^2 = \left(1 - \frac{\Lambda r^2}{3}\right) dt^2 - \left(1 - \frac{\Lambda r^2}{3}\right)^{-1} dr^2 - r^2 d\Omega^2,$$

where  $d\Omega^2$  is the line element on the unit sphere. Main feature of this geometry is divergence of geodesics - in de Sitter geometry gravity effectively acts as a repulsion. Having this in mind, Eddington asked: "May be this is why the Universe is expanding?"

During several next decades, the physical essence of the de Sitter solution remained obscure. In modern physics it has been mainly used as a simple testing ground for developing the quantum field technics in a curved space-time. In 1965 Gliner understood that de Sitter geometry is generated by a vacuum with nonzero energy density [35]. Shifting a cosmological term  $\Lambda g_{\mu\nu}$  from the left-hand side to the right-hand side of Einstein equation (1) corresponds to introducing a stress-energy tensor

$$T_{\mu\nu}^{vac} = (\kappa)^{-1} \Lambda g_{\mu\nu} = \rho_{vac} g_{\mu\nu}; \quad \rho_{vac} = (\kappa)^{-1} \Lambda \quad (2)$$

whose equation of state is

$$p = -\rho_{vac} \quad (3)$$

This stress-energy tensor has an infinite set of comoving reference frames. An observer moving through the medium with the stress-energy tensor (2), cannot in principle measure his velocity with respect to it, since his comoving reference frame is also comoving for  $T_{\mu\nu}^{vac}$  [35].

In 1970 Gliner suggested that de Sitter vacuum can be initial state for an expanding Universe [36]. In 1975 the first nonsingular cosmological model was proposed with the initial de Sitter stage [37]. We have shown that the transition from  $\Lambda$  dominated to the radiation dominated stage produces the growth of the scale factor by about 30 orders of magnitude for the Planck scale vacuum, accompanied by needed growth in the entropy - the result confirmed by all inflationary models involving various mechanisms responsible for  $\Lambda$  (for review see [56]).

Cosmological constant or huge initial vacuum energy density is crucially needed to guarantee surviving of the Universe to its present size and density as well as to explain its observable homogeneity and isotropy [36,37,66,40,50,2]. Inflationary expansion is supposed to begin at the Grand Unification scale of symmetry breaking  $E_{GUT} \sim 10^{15}$  GeV, blowing up a small causally connected region to a size sufficient to explain puzzles of

standard Big Bang cosmology (for review and list of puzzles see, e.g., [43]) - although leaving without explanation the puzzle of cosmological constant itself: *If it was so huge then - how it became so small now?*

### The main puzzle of cosmological constant -

In Quantum Field Theory (QFT), the vacuum stress-energy tensor has the form [16,1,71]

$$\langle T_{\mu\nu} \rangle = \langle \rho_{vac} \rangle g_{\mu\nu}$$

which behaves like an effective cosmological term with  $\Lambda = \kappa \langle \rho_{vac} \rangle$ . In QFT a relativistic field is considered as a collection of harmonic oscillators of all possible frequencies. Vacuum in QFT is a superposition of ground states of all fields. Therefore it has the energy

$$E_{vac} = \sum \frac{1}{2} \hbar \omega, \quad (4)$$

where  $\frac{1}{2} \hbar \omega$  is a zero-point energy of each particular field mode. The expression (4) follows formally from commutation relations which in turn follow from the uncertainty principle applied to a picture of a field as a linear superposition of oscillators. Even for a single harmonic oscillator the uncertainty principle does not allow a particle to be fixed in a state with fixed zero kinetic and zero potential energy. Therefore, for quantum mechanical reasons, zero-point vacuum energy cannot be put equal zero. For aesthetic reasons it could be removed by some subtracting procedure (normal ordering), although it is called back each time when one has to calculate physical effects due to vacuum polarization - for example, Casimir effect [14] which is quite measurable [65].

An upper cutoff for a vacuum energy density is estimated by an energy scale at which our confidence in the formalism of QFT is broken. It is widely believed that it is the Planckian energy  $E_{Pl} \sim 10^{19} \text{ GeV} \sim 10^{16} \text{ erg}$  that marks a point where QFT breaks down due to quantum gravity effects (see, e.g., [45]). It gives

$$\langle \rho_{vac} \rangle \sim 10^{94} \text{ g cm}^{-3} \quad (5)$$

According to General Relativity, a vacuum contributes to gravity by Einstein equations (1). Therefore gravitational influence of a vacuum is not avoidable in principle. With vacuum density (5) its manifestations would be quite dramatic. For example, the cosmic microwave background radiation would have cooled below  $3K$  in the first  $10^{-41} \text{ s}$  after Big Bang, and expansion rate (Hubble parameter) would be about a factor of  $10^{61}$  larger than that observed today [43].

This is the main puzzle of the cosmological constant. According to QFT it must be huge, but according to observations it is for sure very small now. Typically in QFT vacuum energy density is postulated to be zero, in the hope that in future good theory there will be found some cancellation mechanism which zeros out its ultimate

value, or that quantum-cosmological considerations will favor a zero value of cosmological constant [45].

On the other hand, from the cosmological point of view, cosmological constant can not be put equal zero everywhere and forever, since inflation demands it to be huge at the beginning of the Universe evolution, while astronomical data give evidence [45,58,3] that cosmological constant today is comparable with the average density in the Universe

$$\rho_{today} \sim 10^{-30} g \text{ cm}^{-3} \quad (6)$$

### Observational case for a cosmological constant -

The key cosmological parameter to decide if cosmological constant is zero or not today, is the product of the Hubble parameter and the age of the Universe  $H_0 t_0$  (index zero labels values today). For models without cosmological constant it never exceeds 1. In the presence of a nonzero cosmological constant it is possible for the Universe to have this product exceeding 1 (see, e.g., [43]). If Hubble parameter and age of the Universe as measured from high redshift would be found to satisfy the bound  $H_0 t_0 > 1$ , it would require a term in the expansion rate equation that acts as a cosmological constant. Therefore the definitive measurement of  $H_0 t_0 > 1$  would necessitate a non-zero cosmological constant today or the abandonment of standard big bang cosmology [45].

The most pressing piece of data in favour of nonzero cosmological constant involves the estimates of the age of the Universe as compared with the estimates of the Hubble parameter. With taking into account uncertainties in models the best fit to guarantee consensus between all observational constraints is [45,58,3]

$$H_0 = (70 - 80) km \text{ s}^{-1} Mpc^{-1}, \quad t_0 = (13 - 16) \pm 3 Gy,$$

$$\Omega_{matter} = 0.3 - 0.4, \quad \Omega_{\Lambda} = 0.6 - 0.7,$$

where  $\Omega = \rho_{today}/\rho_{cr}$ , and the critical density  $\rho_{cr}$ , which correspond to  $\Omega = 1$ , is given by (6).

Confrontation of models with observations in cosmology as well as the inflationary paradigm, compellingly favour treating the cosmological constant as a variable dynamical quantity .

**$\Lambda$  variability** - The idea that  $\Lambda$  might be variable has been studied for more than two decades (see [1,71] and references therein). In a recent paper on  $\Lambda$ -variability, Overduin and Cooperstock distinguish three approaches [59]. In the first approach  $\Lambda g_{\mu\nu}$  is shifted onto the right-hand side of the field equations (1) and treated as part of the matter content. This approach, originated mainly from Soviet physics school and characterized by Overduin and Cooperstock as connected to dialectic materialism, goes back to Gliner who interpreted  $\Lambda g_{\mu\nu}$  as a vacuum stress-energy tensor, to Zel'dovich who connected  $\Lambda$  with

the gravitational interaction of virtual particles [72], and to Linde who suggested that  $\Lambda$  can vary [49].

In contrast, idealistic approach prefers to keep  $\Lambda$  on the left-hand side of the Eq.(1) and treat it as a constant of nature. The third approach, allowing  $\Lambda$  to vary while keeping it on the left-hand side as a geometrical entity, was first applied by Dolgov in a model in which a classically unstable scalar field, non-minimally coupled to gravity, develops a negative energy density cancelling the initial positive value of a cosmological constant  $\Lambda$  [17].

Whenever variability of  $\Lambda$  is possible, it requires the presence of some matter source other than  $T_{\mu\nu} = (\kappa)^{-1} \Lambda g_{\mu\nu}$ , since the conservation equation  $G^{\mu\nu}_{;\nu} = 0$  implies  $\Lambda = \text{const}$  in this case. This requirement makes it impossible to introduce a cosmological term as variable in itself. However, it is possible for a stress-energy tensor other than  $\Lambda g_{\mu\nu}$ .

In the spherically symmetric case such a possibility is suggested by the Petrov classification scheme [61] and by the Einstein field equations. The algebraic structure of the stress-energy tensor in this case is  $T^r_r = T^t_t$ ;  $T^\theta_\theta = T^\phi_\phi$  [19]. This tensor is invariant under boosts in the radial direction, and describes a spherically symmetric vacuum which represents the extension of the Einstein cosmological term  $\Lambda g_{\mu\nu}$  to the spherically symmetric  $r$ -dependent cosmological tensor  $\Lambda_{\mu\nu}$  [24].

**Nonsingular black hole** - The original motivation for such an extension was to replace a black hole singularity by de Sitter vacuum core. The idea goes back to the 1965 papers by Sakharov who considered the equation of state  $p = -\rho$  as arising at the superhigh densities [63], and by Gliner who suggested that de Sitter vacuum could be a final state in the gravitational collapse [35].

The papers developing this idea appeared in the 80-s as inspired by successes of inflationary paradigm. In those papers direct matching of Schwarzschild metric to the de Sitter metric was considered using thin shell approach [7,30,64]. In this approach the equation of state changes from  $p = 0$ ,  $\rho = 0$  outside to  $p = -\rho_{Pl} \sim 10^{94} g \text{ cm}^{-3}$  within a junction layer of Planckian thickness  $\delta \sim l_{Pl} \sim 10^{-33} cm$ , and the resulting metric has a jump at the junction surface. The situation was analyzed by Poisson and Israel who suggested to insert a layer of a noninflationary material of the uncertain depth at the interface, in which a geometry remains effectively classical and governed by the Einstein equations with a source term representing vacuum polarization effects [62].

The exact analytic solution describing de Sitter-Schwarzschild transition in general case of a distributed density profile, has been found in the Ref [19] in the frame of a simple semiclassical model for a density profile due to vacuum polarization in a spherically symmetric gravitational field [20].

In the case of de Sitter-Schwarzschild transition the variable cosmological term  $\Lambda_{\mu\nu}$  connects in a smooth way

two vacuum states: de Sitter vacuum  $T_{\mu\nu} = (\kappa)^{-1}\Lambda g_{\mu\nu}$  replacing a singularity at the origin, and Minkowski vacuum  $T_{\mu\nu} = 0$  at infinity. For any density profile satisfying the conditions of finiteness of a mass and of a density, the solution to the Einstein equations describes the globally regular de Sitter-Schwarzschild geometry, asymptotically Schwarzschild as  $r \rightarrow \infty$  and asymptotically de Sitter as  $r \rightarrow 0$  [24,20,22]. In the range of masses  $M \geq M_{crit} \simeq 0.3M_{Pl}\sqrt{\Lambda_{Pl}/\Lambda}$  this geometry represents a  $\Lambda$  black hole ( $\Lambda$ BH), while for  $M < M_{cr}$  - a  $\Lambda$  particle, self-gravitating particlelike structure made up of self-gravitating spherically symmetric vacuum  $\Lambda_{\mu\nu}$  [20,24]. In the course of Hawking evaporation of a  $\Lambda$ BH, a second-order phase transition occurs, and globally regular configuration evolves towards a cold remnant which is self-gravitating particlelike structure ( $\Lambda$  particle) at the background of Minkowski or de Sitter space.

In the black hole case the global structure of space-time shows that in place of a former singularity there arises an infinite chain of structures including  $\Lambda$  white holes ( $\Lambda$ WH) and asymptotically flat universes.

**Universes inside a black hole** - The idea of a baby Universe inside a black hole has been proposed by Farhi and Guth (FG) in 1987 [30] as the idea of creation of a universe in the laboratory starting from a false vacuum bubble in the Minkowski space. FG studied an expanding spherical de Sitter bubble separated by thin wall from the outside region where the geometry is Schwarzschild. The global structure of space-time in this case implies that an expanding bubble must be associated with an initial spacelike singularity. The initial singularity clearly represents a singular initial value configuration. Therefore Farhi and Guth concluded that the requirement of initial singularity would be an obstacle to the creation of a universe inside a black hole [30].

In 1990 Farhi, Guth and Guven (FGG) studied the model in which the initial bubble is small enough to be produced without initial singularity [31]. A small bubble classically could not become a universe - instead it would reach a maximum radius and then collapse. FGG investigated the possibility that quantum effects allow the bubble to tunnel into the larger bubble of the same mass which for an external observer disappears beyond the black hole horizon, whereas on the inside the bubble would classically evolve to become a new universe [31].

Arising a new universe inside a black hole has been considered also by Frolov, Markov, and Mukhanov (FMM) in 1989-1990 [33]. The difference of FMM from FG approach is that the FG assumption - the existence of a global Cauchy surface - has been violated, due to the existence of the Cauchy horizon, firstly noticed by Poisson and Israel in 1988 [62], which implies the absence of a global Cauchy surface.

Both FG and FMM models are based on matching Schwarzschild metric outside to de Sitter metric inside

a junction layer of Planckian thickness  $l_{Pl} \sim 10^{-33}$  cm. The case of direct matching clearly corresponds to arising of a closed or semiclosed world inside a black hole [33].

In the case of a distributed density profile - a  $\Lambda$ BH - the dynamical situation is different. The global structure of space-time implies the possibility of existence of an infinite numbers of vacuum-dominated universes inside a  $\Lambda$ BH, and geodesics structure implies possibility of travelling to them. De Sitter vacuum exists near the surface of former singularity  $r = 0$ . This region is the part of a  $\Lambda$ WH, where, as a result of a white hole or de Sitter instability, there is possible quantum creation of baby universes which are disjoint from each other and which can be not only closed, but also open and flat [28].

**Particlelike structure** - In the course of the Hawking evaporation of a  $\Lambda$ BH a second-order phase transition occurs, and a globally regular configuration evolves toward a vacuum-made particlelike structure described by de Sitter-Schwarzschild geometry for the range of masses  $M < M_{crit}$  [20]. Such a configuration can be applied to estimate a lower limit on sizes of fundamental particles (particles which do not display a substructure) [23].

In QFT particles are treated as point-like. Experiments give the upper limits on sizes of fundamental particles (FP) defined by a characteristic size of the region of interaction in the relevant reaction (see review in [23]). One can expect that the lower limits on particle sizes are determined by gravitational interaction [23]. In the case of a FP its gravitational size cannot be defined by the Schwarzschild gravitational radius  $r_g = 2GMc^{-2}$ . Quantum mechanics constrains any size from below by the Planck length  $l_{Pl} \sim 10^{-33}$  cm, and for any elementary particle its Schwarzschild radius is many orders of magnitude smaller than  $l_{Pl}$ .

The Schwarzschild gravitational radius  $r_g$  comes from the Schwarzschild solution which implies a point-like mass and is singular at  $r = 0$ . De Sitter-Schwarzschild geometry represents the nonsingular modification of the Schwarzschild geometry, and depends on the limiting vacuum density  $\rho_{vac}$  at  $r = 0$ . For  $M < M_{cr}$  it describes a neutral self-gravitating particlelike structure with de Sitter vacuum core related to its gravitational mass [20,24]. Now mass is not point-like but distributed, and most of it is within the characteristic size  $\sim (m/\rho_{vac})^{1/3}$ , where  $\rho_{vac}$  is the density at  $r = 0$  [20,21].

In the context of spontaneous symmetry breaking  $\rho_{vac}$  is related to the potential of a scalar field in its symmetric state (false vacuum). In the context of the Einstein-Yang-Mills-Higgs (EYMH) self-gravitating non-Abelian structures including black holes,  $\rho_{vac}$  is related to symmetry restoration in the origin. In a neutral branch of EYMH black hole solutions a non-Abelian structure can be approximated as a sphere of a uniform vacuum density  $\rho_{vac}$  whose radius is the Compton wavelength of the massive non-Abelian field (see [52] and references therein).

Results obtained in the frame of both EYM systems and de Sitter-Schwarzschild geometry suggest that a mass of a FP can be related to a gravitationally induced core with the de Sitter vacuum at  $r = 0$ . We can assume thus that whatever would be a mechanism of a mass generation, a FP must have an internal vacuum core related to its mass and a finite size defined by gravity. With this assumption we are able to set the lower limits on FP sizes by sizes of their vacuum cores as defined by de Sitter-Schwarzschild geometry. It gives us also an upper limit on the mass of a Higgs scalar [23].

**Structure of this paper** - This paper summarizes our results on variable cosmological term  $\Lambda_{\mu\nu}$  in the spherically symmetric case. It is organized as follows. The  $r$ -dependent cosmological term  $\Lambda_{\mu\nu}$  is introduced in Section II. In Section III we present de Sitter-Schwarzschild geometry including both black hole sector and particlelike sector. In Section IV we outline our results on two-lambda geometry which is the extension of de Sitter-Schwarzschild geometry to the case of nonzero value of cosmological constant at infinity.

## II. COSMOLOGICAL TERM $\Lambda_{\mu\nu}$

In the spherically symmetric static case a line element can be written in the form [67]

$$ds^2 = e^{\mu(r)} dt^2 - e^{\nu(r)} dr^2 - r^2 d\Omega^2 \quad (7)$$

where  $d\Omega^2$  is the line element on the unit sphere. The Einstein equations read

$$\kappa T_t^t = e^{-\nu} \left( \frac{\nu'}{r} - \frac{1}{r^2} \right) + \frac{1}{r^2} \quad (8)$$

$$\kappa T_r^r = -e^{-\nu} \left( \frac{\mu'}{r} + \frac{1}{r^2} \right) + \frac{1}{r^2} \quad (9)$$

$$\kappa T_\theta^\theta = 8\pi G T_\phi^\phi =$$

$$-e^{-\nu} \left( \frac{\mu''}{2} + \frac{\mu'^2}{4} + \frac{\mu' - \nu'}{2r} - \frac{\mu'\nu'}{4} \right) \quad (10)$$

A prime denotes differentiation with respect to  $r$ . In the case of

$$T_{\mu\nu} = \kappa^{-1} \Lambda g_{\mu\nu} = \rho_{vac} g_{\mu\nu} \quad (11)$$

the solution is the de Sitter geometry with constant positive curvature  $R = 4\Lambda$ . The line element is

$$ds^2 = \left( 1 - \frac{\Lambda r^2}{3} \right) dt^2 - \left( 1 - \frac{\Lambda r^2}{3} \right)^{-1} dr^2 - r^2 d\Omega^2 \quad (12)$$

There is the causal horizon in this geometry defined by

$$r_0^2 = \frac{3}{\Lambda} = \frac{3}{\kappa \rho_{vac}} \quad (13)$$

The algebraic structure of the stress-energy tensor, corresponding to a cosmological term  $\Lambda g_{\mu\nu}$ , is

$$T_t^t = T_r^r = T_\theta^\theta = T_\phi^\phi; \quad p = -\rho \quad (14)$$

In the Petrov classification scheme [61] stress-energy tensors are classified on the basis of their algebraic structure. When the elementary divisors of the matrix  $T_{\mu\nu} - \beta g_{\mu\nu}$  (i.e., the eigenvalues of  $T_{\mu\nu}$ ) are real, the eigenvectors of  $T_{\mu\nu}$  are nonisotropic and form a comoving reference frame. Its timelike vector represents a velocity. The classification of the possible algebraic structures of stress-energy tensors satisfying the above conditions contains five possible types: [III], [I(III)], [(II)(II)], [(II)(II)], [(III)]. The first symbol denotes the eigenvalue related to the timelike eigenvector. Parentheses combine equal (degenerate) eigenvalues. A comoving reference frame is defined uniquely if and only if none of the spacelike eigenvalues  $\beta_\alpha$  ( $\alpha = 1, 2, 3$ ) coincides with a timelike eigenvalue  $\beta_0$ . Otherwise there exists an infinite set of comoving reference frames.

In this scheme the de Sitter stress-energy tensor (11) is represented by [(III)] (all eigenvalues being equal) and classified as a vacuum tensor due to the absence of a preferred comoving reference frame [35]. In the spherically symmetric case it is possible, by the same definition, to introduce an  $r$ -dependent vacuum stress-energy tensor with the algebraic structure [19]

$$T_t^t = T_r^r; \quad T_\theta^\theta = T_\phi^\phi \quad (15)$$

In the Petrov classification scheme this stress-energy tensor is denoted by [(II)(II)]. It has an infinite set of comoving reference frames, since it is invariant under rotations in the  $(r, t)$  plane. Therefore an observer moving through it cannot in principle measure the radial component of his velocity. The stress-energy tensor (15) describes a spherically symmetric anisotropic vacuum invariant under the boosts in the radial direction [19].

The conservation equation  $T^{\mu\nu}_{;\nu} = 0$  gives the  $r$ -dependent equation of state [62,19]

$$p_r = -\rho; \quad p_\perp = p_r + \frac{r}{2} \frac{dp_r}{dr}, \quad (16)$$

where  $\rho = T_t^t$  is the density,  $p_r = -T_r^r$  is the radial pressure, and  $p_\perp = -T_\theta^\theta = -T_\phi^\phi$  is the tangential pressure. In this case equations (7)-(8) reduce to the equation

$$\kappa \rho = e^{-\nu} \left( \frac{\nu'}{r} - \frac{1}{r^2} \right) + \frac{1}{r^2} \quad (17)$$

whose solution is

$$g_{00} = e^{-\nu(r)} = 1 - \frac{2G\mathcal{M}(r)}{r}; \quad \mathcal{M}(r) = 4\pi \int_0^r \rho(x) x^2 dx \quad (18)$$

and the line element is given by

$$ds^2 = \left(1 - \frac{2GM(r)}{r}\right) dt^2 - \left(1 - \frac{2GM(r)}{r}\right)^{-1} dr^2 - r^2 d\Omega^2 \quad (19)$$

If we require the density  $\rho(r)$  to vanish as  $r \rightarrow \infty$  quicker than  $r^{-3}$ , then the metric (19) for large  $r$  has the Schwarzschild form

$$ds^2 = \left(1 - \frac{2GM}{r}\right) dt^2 - \left(1 - \frac{2GM}{r}\right)^{-1} dr^2 - r^2 d\Omega^2 \quad (20)$$

with

$$M = 4\pi \int_0^\infty \rho(r) r^2 dr < \infty \quad (21)$$

If we impose the boundary condition of de Sitter behaviour (12) at  $r \rightarrow 0$ , the form of the mass function  $\mathcal{M}(r)$  in the limit of small  $r$  must be

$$\mathcal{M}(r) = \frac{\Lambda}{6G} r^3 = \frac{4\pi}{3} \rho_{vac} r^3 \quad (22)$$

For any density profile satisfying conditions (21)-(22), the metric (19) describes a globally regular de Sitter-Schwarzschild geometry, asymptotically Schwarzschild as  $r \rightarrow \infty$  and asymptotically de Sitter as  $r \rightarrow 0$  [20,22].

The stress-energy tensor (15) responsible for this geometry connects in a smooth way two vacuum states: de Sitter vacuum (11) at the origin and Minkowski vacuum  $T_{\mu\nu} = 0$  at infinity. The inflationary equation of state  $p = -\rho$  remains valid for the radial component of a pressure. This makes it possible to treat the stress-energy tensor (15) as corresponding to an  $r$ -dependent cosmological term  $\Lambda_{\mu\nu}$ , varying from  $\Lambda_{\mu\nu} = \Lambda g_{\mu\nu}$  as  $r \rightarrow 0$  to  $\Lambda_{\mu\nu} = 0$  as  $r \rightarrow \infty$ , and satisfying the equation of state (16) with  $\rho^\Lambda = \Lambda_t^\Lambda$ ,  $p_r^\Lambda = -\Lambda_r^\Lambda$  and  $p_\perp^\Lambda = -\Lambda_\theta^\Lambda = -\Lambda_\phi^\Lambda$ .

If we modify the density profile to allow a non-zero value of cosmological constant  $\lambda$  as  $r \rightarrow \infty$ , putting

$$T_t^t(r) = \rho(r) + \kappa^{-1}\lambda, \quad (23)$$

we obtain the metric [25]

$$ds^2 = \left(1 - \frac{2G\mathcal{M}(r)}{r} - \frac{\lambda r^2}{3}\right) dt^2 - \left(1 - \frac{2G\mathcal{M}(r)}{r} - \frac{\lambda r^2}{3}\right)^{-1} dr^2 - r^2 d\Omega^2 \quad (24)$$

whose asymptotics are the de Sitter metric (12) with  $\lambda$  as  $r \rightarrow \infty$  and with  $(\Lambda + \lambda)$  as  $r \rightarrow 0$ .

The stress-energy tensor responsible for two-lambda geometry connects in a smooth way two vacuum states with non-zero cosmological constant: de Sitter vacuum  $T_{\mu\nu} = \kappa^{-1}(\Lambda + \lambda)g_{\mu\nu}$  at the origin, and de Sitter vacuum  $T_{\mu\nu} = \kappa^{-1}\lambda g_{\mu\nu}$  at infinity. This confirms the interpretation of the stress-energy tensor with the algebraic structure (15) as corresponding to a variable effective cosmological term  $\Lambda_{\mu\nu}$  [24].

### III. DE SITTER-SCHWARZSCHILD GEOMETRY

#### A. Horizons and objects

De Sitter-Schwarzschild geometry (19) belongs to the class of solutions to the Einstein equations (8)-(10) with the source term  $T_\mu^\nu$  of the algebraic structure (15). Formally it follows from imposing the condition  $g_{00} = -g_{11}^{-1}$  on the metric [19]. This condition applied to the system of equations (8)-(10), follows in the condition  $T_t^t = T_r^r$  which defines the class of spherically symmetric geometries generated by a variable cosmological term  $\Lambda_\mu^\mu$ . De Sitter-Schwarzschild geometry is the member of this class, distinguished by the boundary conditions of de Sitter behaviour (12) at  $r = 0$  and Schwarzschild behaviour (20) at infinity.

All the main features of this geometry follow from the algebraic structure of a source term  $\Lambda_{\mu\nu}$  and from the imposed boundary conditions, independently of physical mechanism responsible for  $\Lambda_{\mu\nu}$ , in the same way as all the main features of de Sitter geometry are defined by the Einstein cosmological term  $\Lambda g_{\mu\nu}$ , independently on physical mechanisms responsible for cosmological constant.

The fundamental difference from the Schwarzschild case is that for any density profile satisfying (21)-(22), there are two horizons, a black hole horizon  $r_+$  and an internal Cauchy horizon  $r_-$  [62,33,19]. A black hole horizon is formed by outgoing radial photon geodesics - zero generators of a horizon. The Cauchy horizon consists of ingoing radial photon geodesics which are not extendible to the past. Therefore a global Cauchy surface does not exist in this geometry.

Horizons are calculated as the positive roots of the equation  $g_{00}(r) = 0$ . In the de Sitter-Schwarzschild geometry horizons exist for the masses in the region  $M \leq M_{crit}$ . A critical value of the mass  $M_{crit}$  marks the point at which the horizons come together. It gives the lower limit for a black hole mass.

Horizons are plotted in Fig.1 for the case of the density profile described by the Schwinger formula for the vacuum polarization [55] in the spherically symmetric gravitational field which gives [19,20]

$$\rho(r) = \kappa^{-1}\Lambda \exp\left(-\frac{\Lambda}{6GM}r^3\right) = \rho_{vac} \exp\left(-\frac{4\pi}{3}\frac{\rho_{vac}}{M}r^3\right) \quad (25)$$

The mass function in the metric (19) then takes the form

$$\mathcal{M}(r) = M \left(1 - \exp\left(-\frac{\Lambda}{6GM}r^3\right)\right) \quad (26)$$

The lower limit for a  $\Lambda$ BH mass is given by

$$M_{crit} \simeq 0.3 M_{Pl} (\Lambda_{Pl}/\Lambda)^{1/2} \quad (27)$$

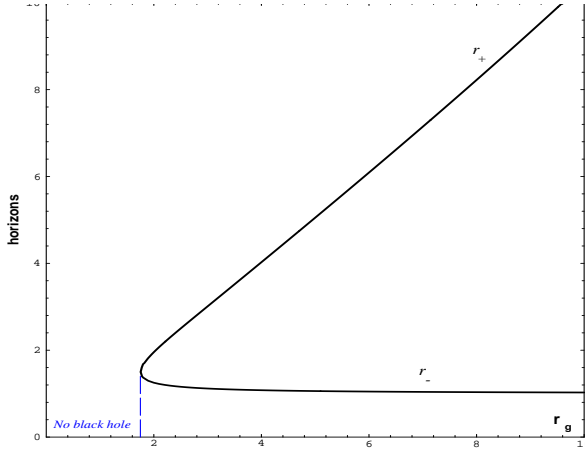


FIG. 1. Horizons of de Sitter-Schwarzschild geometry plotted in the case of the density profile (25).

Depending on the value of the mass  $M$ , there exist three types of configurations in which a Schwarzschild singularity is replaced with  $\Lambda$  core [20,22]: 1) a  $\Lambda$  black hole for  $M > M_{crit}$ ; 2) an extreme  $\Lambda$ BH for  $M = M_{crit}$ ; 3) a "  $\Lambda$  particle" ( $\Lambda$ P) - a particlelike structure without horizons made up of a self-gravitating spherically symmetric vacuum (15) - for  $M < M_{crit}$ .

De Sitter-Schwarzschild configurations are plotted in Fig.2 for the case of the density profile (25).

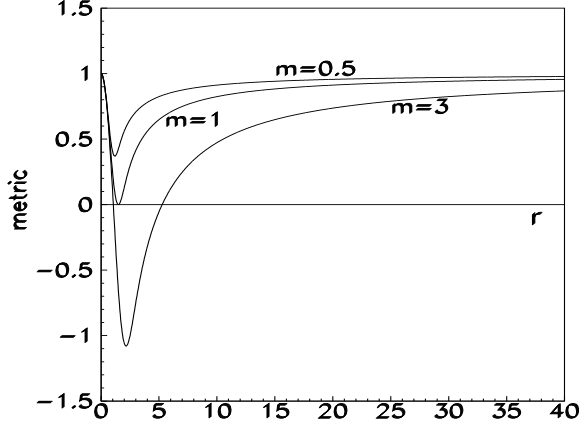


FIG. 2. The metric coefficient  $g_{00}(r)$  for de Sitter-Schwarzschild configurations in the case of the density profile (25). The parameter  $m$  is the mass  $M$  normalized to  $M_{crit} \simeq 0.3M_{Pl}(\Lambda_{Pl}/\Lambda)^{1/2}$ .

The question of the stability of a  $\Lambda$ BH and  $\Lambda$ P is currently under investigation. Comparison of the ADM mass (21) with the proper mass  $\mu$  which is the sum of the invariant masses of all particles [53]

$$\mu = 4\pi \int \rho(r)(1 - 2GM(r)/r)^{-1/2} r^2 dr \quad (28)$$

gives us a hint. In the spherically symmetric situations the ADM mass represents the total energy,  $M = \mu + \text{binding energy}$  [53]. In our case  $\mu$  is bigger than  $M$ . This suggests that the configuration might be stable since energy is needed to break it up [24].

## B. Black and white holes

The global structure of de Sitter-Schwarzschild space-time in the case  $M > M_{crit}$  is shown in Fig.3 [20]. It contains an infinite sequence of black and white holes whose singularities are replaced with future and past de Sitter regular cores  $\mathcal{RC}$ , and asymptotically flat universes  $\mathcal{U}$ . Penrose-Carter diagram is plotted in coordinates of the photon radial geodesics. The surfaces  $\mathcal{J}^-$  and  $\mathcal{J}^+$  are their past and future infinities. The surfaces  $i^0$  are space-like infinities. The event horizons  $r_+$  and the Cauchy horizons  $r_-$  are formed by the outgoing and ingoing radial photon geodesics  $r_{\pm} = \text{const.}$

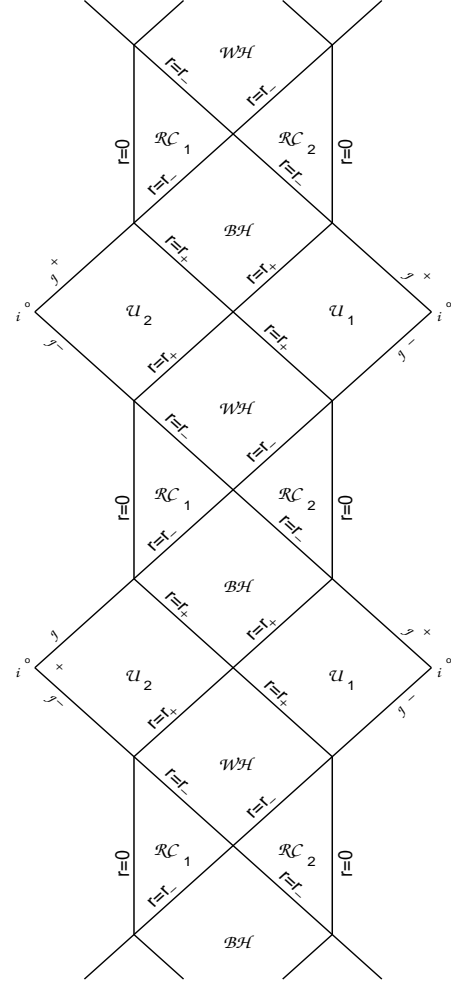


FIG. 3. Penrose-Carter diagram for  $\Lambda$  black hole.

It is evident from the Penrose-Carter diagram for  $\Lambda$ BH that inside it there exists an infinite number of vacuum-dominated asymptotically flat universes in the future of  $\Lambda$  white holes. Geodesic structure of de Sitter-Schwarzschild space-time shows that the possibility of travelling into other universes through a black hole interior, discussed in the literature for the case of Reissner-Nordstrom and Kerr geometry (see, e.g., [55]), exists also in the case of a  $\Lambda$ BH as the opportunity of safe travel - without a risk to get into a singularity [27].

**A white hole model for nonsimultaneous big bang-** It is widely known that the interiors of black and white holes can be described locally as cosmological models (see, e.g., [46]). In the case of a Schwarzschild white hole it starts from the spacelike singularity  $r = 0$  (see Fig.4).

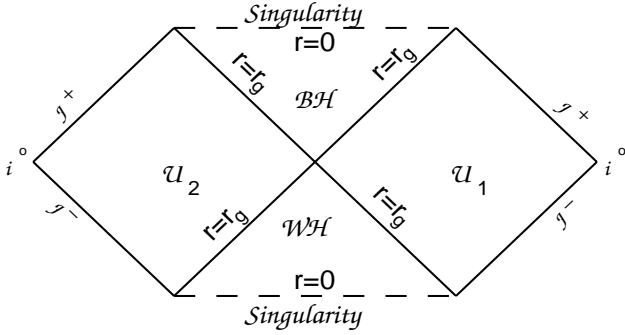


FIG. 4. Penrose-Carter diagram for the Schwarzschild black hole.

Replacing a Schwarzschild singularity with the regular core  $\mathcal{RC}$  transforms the spacelike singular surfaces  $r = 0$ , both in the future of a  $\mathcal{BH}$  and in the past of a  $\mathcal{WH}$ , into the timelike regular surfaces (see Fig.3). In a sense, this rehabilitates a white hole whose existence in a singular version has been forbidden by the cosmic censorship [60].

Cosmological model related to a  $\Lambda$ WH corresponds to asymptotically flat vacuum-dominated cosmology with the de Sitter origin, governed by the time-dependent cosmological term  $\Lambda_\mu^\nu$  (segment  $\mathcal{RC}$ ,  $\mathcal{WH}$ ,  $\mathcal{U}$  in the Fig.3). A  $\Lambda$ WH models thus initial stages of nonsingular cosmology with an inflationary origin.

To investigate a  $\Lambda$ WH together with its past regular core  $\mathcal{RC}$  and future asymptotically flat universe  $\mathcal{U}$ , we transform Schwarzschild coordinates  $(t, r)$  into Finkelstein coordinates  $(\tau, R)$  related to radial geodesics of test particles at rest at infinity

$$c\tau = \pm ct \pm \int \sqrt{\frac{R_g(r)}{r} + f(R)} \frac{dr}{1 - \frac{R_g(r)}{r}}, \quad (29)$$

$$R = ct + \int \sqrt{\frac{r}{R_g(r)}} \frac{\sqrt{1 + f(R)} dr}{1 - \frac{R_g(r)}{r}} \quad (30)$$

Here

$$R_g(r) = \frac{2GM(r)}{c^2} \quad (31)$$

and  $f(R)$  is an arbitrary function satisfying the condition  $1 + f(R) > 0$ . The lower sign in (29) is for outgoing geodesics corresponding to the case of an expansion.

The metric (19) transforms into the Lemaitre type metric [46]

$$ds^2 = c^2 d\tau^2 - e^{\lambda(R, \tau)} dR^2 - r^2(R, \tau) d\Omega^2 \quad (32)$$

with

$$e^{\lambda(R, \tau)} = \frac{R_g(r(R, \tau))}{r(R, \tau)}$$

Coordinates  $R, \tau$  are the Lagrange (comoving) coordinates of a test particle, and  $r$  is its Euler radial coordinate (luminosity distance). In the case of outgoing geodesics the  $(R, \tau)$  coordinates with the lower sign in (29), map the segment  $\mathcal{RC}, \mathcal{WH}, \mathcal{U}$ , i.e. a  $\Lambda$ WH together with its past regular core  $\mathcal{RC}$  and an external universe  $\mathcal{U}$  in its absolute future.

For the metric (32) the Einstein equation reduce to [46]

$$\kappa p_r = \frac{1}{r^2} (e^{-\lambda} r'^2 - 2r\ddot{r} - \dot{r}^2 - 1) \quad (33)$$

$$\kappa p_\perp = \frac{e^{-\lambda}}{r} \left( r'' - \frac{r'\lambda'}{2} \right) - \frac{\dot{r}\dot{\lambda}}{2r} - \frac{\ddot{\lambda}}{2} - \frac{\dot{\lambda}^2}{4} - \frac{\ddot{r}}{r} \quad (34)$$

$$\kappa \rho = -\frac{e^{-\lambda}}{r^2} (2rr'' + r'^2 - rr'\lambda') + \frac{1}{r^2} (r\dot{r}\dot{\lambda} + \dot{r}^2 + 1) \quad (35)$$

$$\kappa T_t^r = \frac{e^{-\lambda}}{r} (2\dot{r}' - r'\dot{\lambda}) = 0 \quad (36)$$

Here the dot denotes differentiation with respect to  $\tau$  and  $'$  with respect to  $R$ . The component  $T_t^r$  of the stress-energy tensor vanishes in the comoving reference frame, and the Eq.(36) is integrated giving [46]

$$e^\lambda = \frac{r'^2}{1 + f(R)} \quad (37)$$

Then we obtain from Eq.(33) the equation of motion

$$\dot{r}^2 + 2r\ddot{r} + \kappa p_r r^2 = f(R) \quad (38)$$

This cosmological model belongs to the Lemaitre class of spherically symmetric models with anisotropic fluid [48]. Dynamics of our model is governed by cosmological tensor  $\Lambda_{\mu\nu}$  which in this case is time-dependent. For numerical integration of the equation of motion we adopt the density profile (25). Behavior of pressures  $p_r^\Lambda = -\Lambda_r^r$  and  $p_\perp^\Lambda = -\Lambda_\theta^\theta = -\Lambda_\phi^\phi$  in this case is shown in Fig.5.



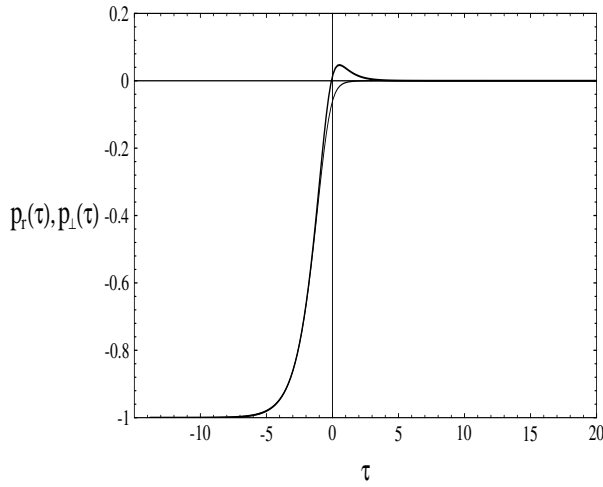


FIG. 5. Radial and tangential pressures  $p_r < p_t$ .

Near the surface  $r = 0$  the metric (32) transforms into the FRW form with de Sitter scale factor for any  $f(R)$ . The further evolution of geometry is calculated numerically. Here we present numerical results for the case of  $f(R) = 0$  [28] which correspond to the most popular today cosmological model with  $\Omega = 1$ .

The characteristic scale of de Sitter-Schwarzschild space-time is  $r_* = (r_0^2 r_g)^{1/3}$ , and we normalize  $r$  to this scale introducing dimensionless variable  $\xi$  by  $r = r_* \xi$ . The equation of motion (38) for  $f(R) = 0$  reduces to

$$\dot{\xi}^2 + 2\xi\ddot{\xi} - 3\xi^2 e^{-\xi^3} = 0 \quad (39)$$

It has the first integral

$$\dot{\xi}^2 = \frac{A - e^{-\xi^3}}{\xi} \quad (40)$$

and the second integral

$$\tau - \tau_0(R) = \int_{\xi_0}^{\xi} \sqrt{\frac{x}{A - e^{-x^3}}} dx \quad (41)$$

Here  $\tau_0(R)$  is an arbitrary function (constant of integration parametrized by  $R$ ) which is called the "bang-time function" [57]. For example, in the case of the Tolman-Bondi model for a dust (an ideal non-zero rest mass pressureless gas), the evolution is described by  $r(R, \tau) = (9GM(R)/2)^{1/3} (\tau - \tau_0(R))^{2/3}$ , where  $\tau_0(R)$  is an arbitrary function of  $R$  representing the big bang singularity surface for which  $r(R, \tau) = 0$  [15].

The bang starts from  $\xi_0 = 0$  which is timelike regular surface (see Fig.3). Choosing  $\xi_0 = 0$  we fix the constant  $A = 1$  and  $\tau_0(R) = -R$ . In coordinates  $(R, \tau)$  bang starts from the surface  $R + c\tau = -\infty$  shown in the Fig.6.

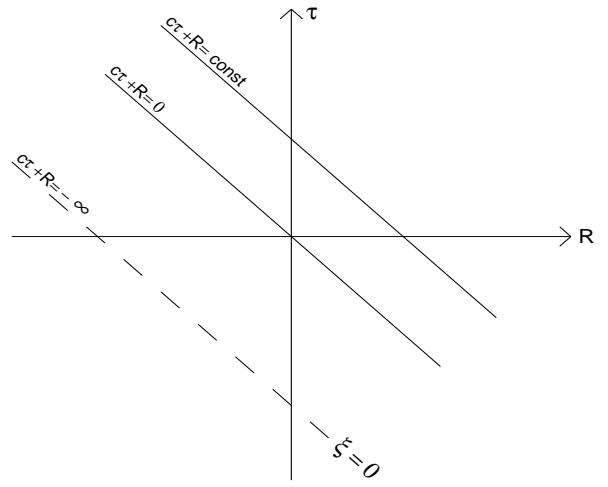


FIG. 6. Surfaces  $r = \text{const}$  plotted for dimensionless radius  $\xi$ . The surface  $\xi = 0$  is the big bang surface.

Different points of the bang surface  $\xi = 0$  start at different moments of synchronous time  $\tau$ . In the limit  $\xi \rightarrow 0$ , the metric takes the form

$$ds^2 = c^2 d\tau^2 - r_0^2 e^{\frac{2c\tau}{r_0}} (dq^2 + q^2 d\Omega^2) \quad (42)$$

where the variable  $q = e^{\frac{R}{r_0}}$  is introduced to transform the metric (32) into the FRW form. It describes, with the initial conditions  $\xi_0(R + \tau \rightarrow -\infty) = 0$ ,  $\dot{\xi}_0(R + \tau \rightarrow -\infty) = 0$ , the nonsingular nonsimultaneous de Sitter bang.

In the case of a Schwarzschild WH, a singularity is spacelike (see Fig.4), so there exist the reference frame in which it is simultaneous. In the case of a  $\Lambda$  white hole, a surface  $r = 0$  is timelike (Fig.3), and there does not exist any reference frame in which two events occurring on  $r = 0$  would be simultaneous.

The first lesson of the  $\Lambda$ WH model is that nonsingular big bang must be nonsimultaneous [28].

The further evolution of the function  $\xi$ , velocity  $\dot{\xi}$  and acceleration  $\ddot{\xi}$  is shown in Figs 7-9, obtained by numerical integration of the equation of motion (39) with the initial conditions  $\xi_0 = 10^{-6}$ ,  $\dot{\xi}_0 = 10^{-6}$  [28].

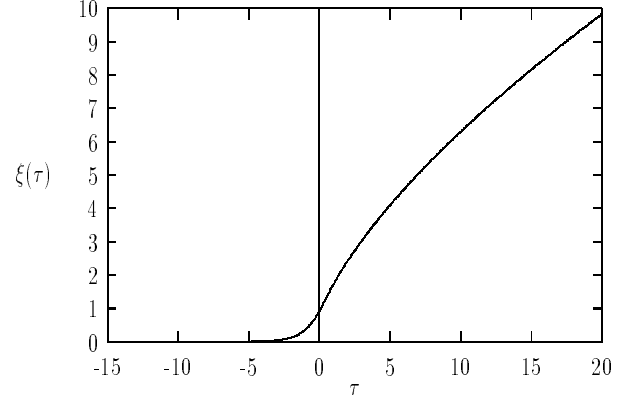


FIG. 7. The function  $\xi(\tau - \tau_0)$  calculated from Eq.(39) with initial conditions  $\xi_0 = \dot{\xi}_0 = 10^{-6}$ .

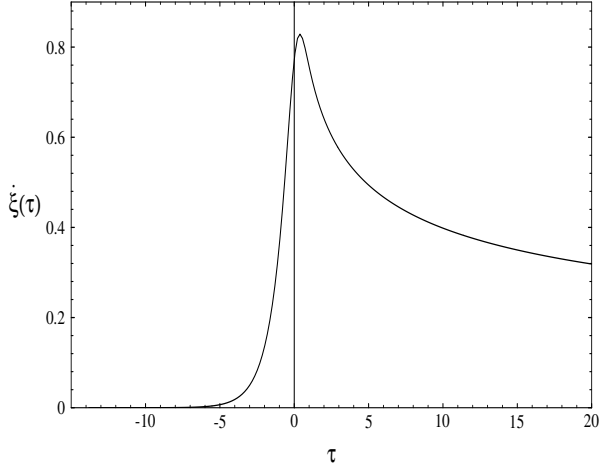


FIG. 8. The plot of the velocity  $\dot{\xi}(\tau - \tau_0)$  for initial conditions  $\xi_0 = \dot{\xi}_0 = 10^{-6}$ .

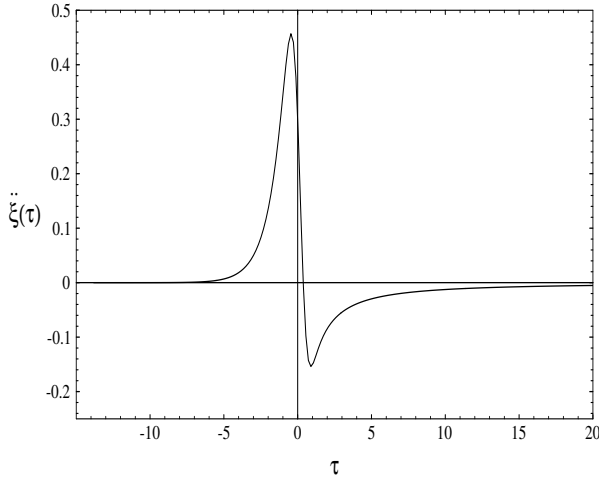


FIG. 9. The acceleration of the "scale factor"  $\xi(\tau - \tau_0)$ .

Numerical integration of the equation (39) shows exponential growth of  $\xi(\tau - \tau_0)$  at the beginning, when  $p_\perp \simeq p_r \simeq -\rho$ , followed by anisotropic Kasner-type stage when different pressures lead to anisotropic expansion.

Qualitatively we can see this approximating the second integral (41) in the region  $1 \ll \xi \ll (r_g/r_0)^{2/3}$  (far beyond a  $\Lambda$ WH horizon) by

$$ds^2 = c^2 d\tau^2 - \left(\frac{9r_g}{4}\right)^{\frac{2}{3}} (\tau + \tilde{\tau}_0(R))^{-\frac{2}{3}} \left(\frac{d\tilde{\tau}_0(R)}{dR}\right)^2 dR^2 - \left(\frac{9r_g}{4}\right)^{\frac{2}{3}} (\tau + \tilde{\tau}_0(R))^{\frac{2}{3}} d\Omega^2 \quad (43)$$

where  $\tilde{\tau}_0(R) = R + \left(\frac{2}{3}\xi_0^{\frac{2}{3}}(R) - F(\xi_0(R))\right)$  and  $F(\xi_0(R)) = \int_0^{\xi_0(R)} \sqrt{\frac{x}{1-e^{-x^3}}} dx$ .

This is anisotropic Kasner-type metric, with contraction in the radial direction, and expansion in the tangential direction. Our model here differs from the Kasner vacuum solution by nonzero anisotropic pressures.

The second lesson of the  $\Lambda$ WH model is the existence of the anisotropic Kasner-type stage after inflation.

This stage follows the nonsingular nonsimultaneous big bang from the regular surface  $r = 0$ . It looks that this kind of behaviour is generic for cosmological models near the origin [4] (for recent review see [6]). Our case differs from singular case also in that our solution displaying Kasner-type stage is not vacuum in the sense of zero right-hand side of the Einstein equations. However it is still vacuum-dominated in the sense that the cosmological term  $\Lambda_{\mu\nu}$  corresponds to a spherically symmetric vacuum.

Since in our  $\Omega = 1$  model 3-curvature is zero, ADM mass  $\mathcal{M}$  given by (18), coincides with the total proper mass  $\mu$  given by (28) as the sum of the invariant masses of all particles with radial coordinate less than a certain value of  $R$ , frequently referred to as the Bondi mass [9]. At the beginning  $\mathcal{M} = 0$  and  $\dot{\mathcal{M}} = 0$ , as it follows from the first integral (40) which gives [28]

$$\dot{\xi}^2 = \frac{\mathcal{M}(\xi)}{\xi} \quad (44)$$

The behavior of mass normalized to Schwarzschild mass  $M$  is shown in the Fig.10.

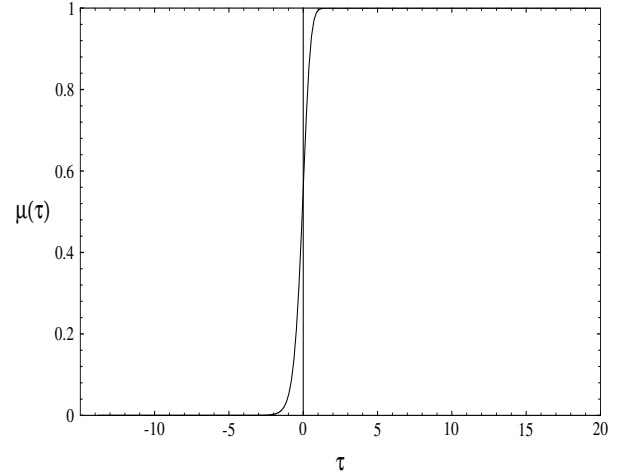


FIG. 10. Plot of the mass function  $\mu = \mathcal{M}/M$ .

At the inflationary stage the mass increases as  $\xi^3$ . At the next anisotropic stage it is growing abruptly towards the value of the Schwarzschild mass  $M$ . Since the density is quickly falling at the some time starting from the initial value  $\rho_{vac} = \kappa^{-1}\Lambda$ , the growth in a mass is connected with the fall of  $\rho^\Lambda = \Lambda_t^t$ , i.e., with the decay of the initial vacuum energy (as it was noted in the Ref [37]).

The third lesson of  $\Lambda$ WH model - quick growth of the mass during the Kasner-type anisotropic stage.

**Baby universes inside a  $\Lambda$ BH** - In the case of direct matching of de Sitter to Schwarzschild metric [30,33] the global structure of space-time corresponds to arising of a closed or semiclosed world [33] inside a BH (Fig.11).

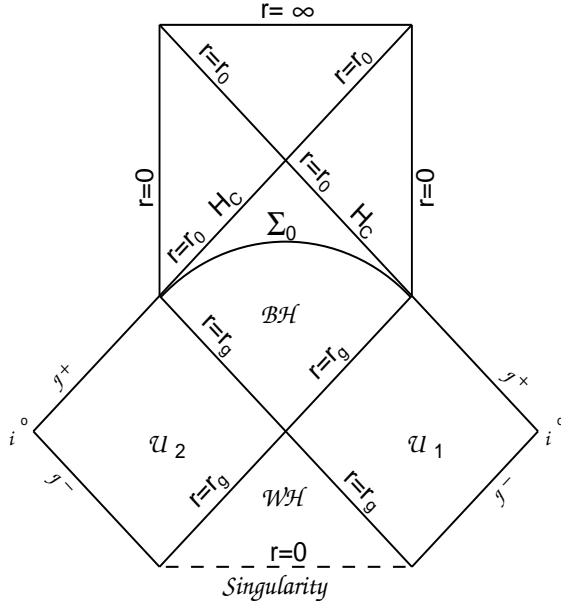


FIG. 11. Penrose-Carter diagram for the case of the direct de Sitter-Schwarzschild matching.

The conformal diagram shown in Fig.3 represents the global structure of de Sitter-Schwarzschild spacetime in general case of a distributed density profile. The situation near the surface  $r = 0$  is similar to the case considered by Farhi and Guth [30,31]. The region near  $r = 0$ , which is the part of the regular core  $\mathcal{RC}$ , differs from that considered in Ref. [31] by an  $r$ -dependent density profile. Our density profile (25) is almost constant near  $r \rightarrow 0$  and then quickly falls down to zero. In Fig.12 it is plotted for the case of a stellar mass black hole with  $M = 3M_{\odot}$ .

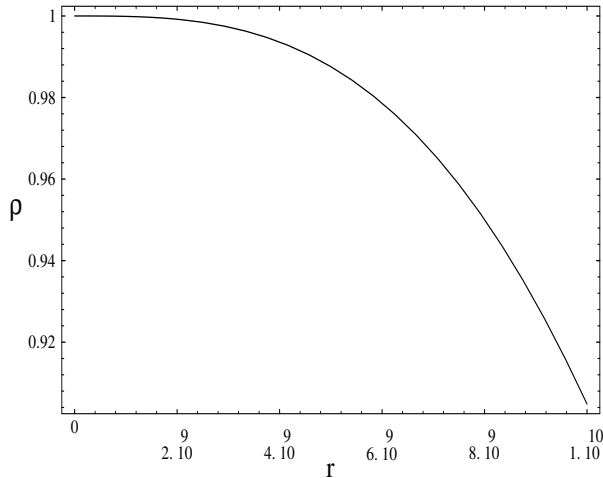


FIG. 12. Density profile (25) for the case of three solar masses nonsingular black hole.

We may think of the region near  $r = 0$  as of a small false vacuum bubble which can be a seed for a quantum birth of a new universe. In this context quantum creation of a baby universe inside a  $\Lambda$ BH would change the global structure of spacetime as it is shown in Fig.13, which corresponds to arising of a closed or semiclosed world in one of  $\Lambda$ WH structures in the future of a  $\Lambda$ BH in the original universe.

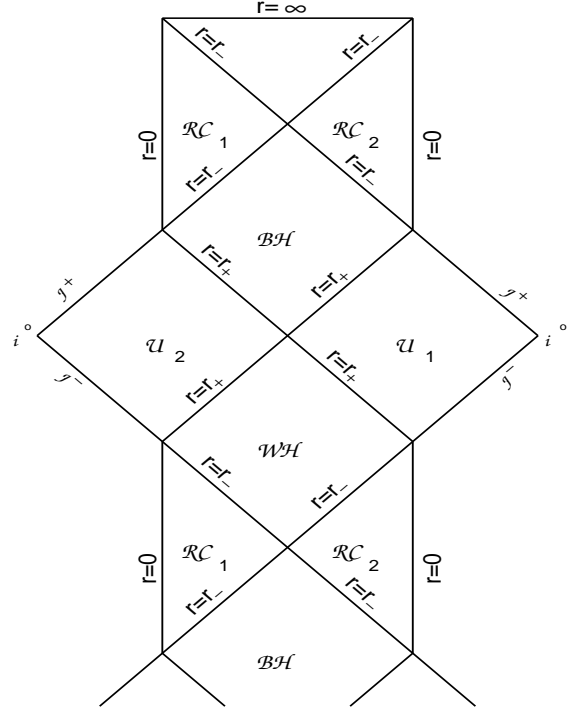


FIG. 13. The global structure of space-time for the case of creation of closed or semiclosed universe inside a  $\Lambda$  black hole.

On the other hand, in the case of a  $\Lambda$ BH with a distributed density profile, whose global structure (Fig.3) is essentially different from that of direct matching case (Fig.11), there exist possibilities other than considered by Farhi and Guth.

It has been well known since the very beginning of studying white holes that they are unstable. Instabilities of Schwarzschild white holes are related to physical processes (particle creation) near a singularity (see [55] and references therein). In the case of a  $\Lambda$ WH its quantum instability is related to instability of de Sitter vacuum near the surface  $r = 0$ . Therefore we can consider arising of a baby universe in a  $\Lambda$ BH as the result of quantum instability of de Sitter vacuum.

Instability of de Sitter vacuum is well studied, both with respect to particle creation (see [8,39]), and with respect to quantum birth of a universe [37,38,50,2,69,70,51,56]. The possibility of birth of a universe from de Sitter vacuum has been widely discussed in the literature.

The possibility of multiple birth of causally disconnected universes from de Sitter background has been noticed in our 1975 paper [37]. In 1982 such a possibility has been investigated by J. Richard Gott III who considered creation of a universe as a quantum barrier penetration leading to an open FRW cosmology [38]. Linde [50] and Albrecht and Steinhardt [2] have suggested detailed mechanisms for forming bubbles, and now these single-bubble models are spoken of as the "new inflationary scenario" (for review see [51]).

The case of arising of an open or flat universe from de Sitter vacuum is illustrated by Fig.14 from J. Richard Gott III paper [38]. The events  $E$  and  $E'$  are birth of causally disconnected universes (open in Gott III case) from de Sitter vacuum. The curved lines are world lines of comoving observers. At the spacelike surface  $AB$  the phase transition occurs from the inflationary  $p = -\rho$  stage to the radiation dominated  $p = \rho/3$  stage [37,38].

In the case of a  $\Lambda$ BH the region  $ECB$  in Fig.14 corresponds to the region  $\mathcal{RC}_1$  in Fig.3, and the region  $BFD$  corresponds to the part of region  $\mathcal{RC}_2$ . Those two regions in de Sitter-Schwarzschild space-time are entirely disjoint from each other for the same reasons as the regions  $\mathcal{U}_1$  and  $\mathcal{U}_2$  (they can be connected only by spacelike curves). Birth of baby universes inside a  $\Lambda$ BH looks very similar to the picture shown in Fig.14.

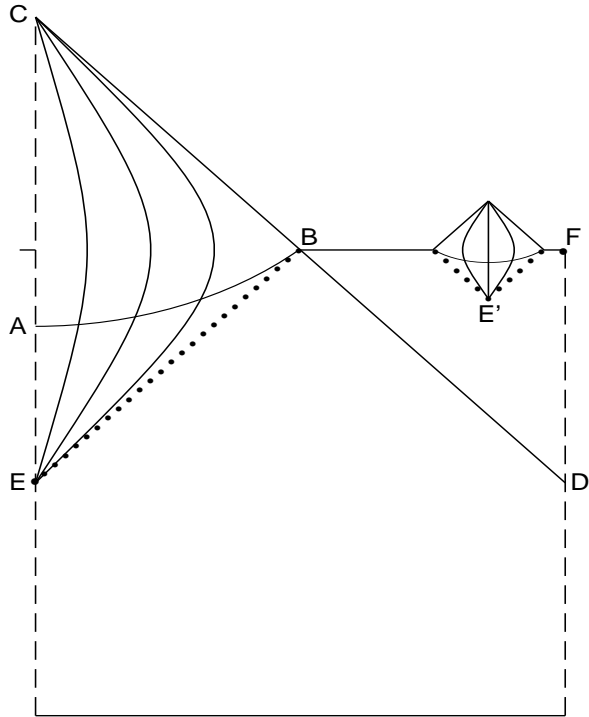


FIG. 14. Penrose-Carter diagram [38], which corresponds to the case of birth of baby universes inside a  $\Lambda$ BH [28].

In any case a nucleating bubble is spherical and can be described by a minisuperspace model with a single degree of freedom [70], in our case  $a = (r_0^2 r_g)^{1/3} \xi$ .

The Friedmann equation in the conformal time ( $cdt = ad\eta$ ) reads

$$\left(\frac{da}{d\eta}\right)^2 = \frac{8\pi G \rho a^4}{3c^2} - k a^2, \quad (45)$$

where  $k = 0, \pm 1$ . Standard procedure of quantization [69,70] results in the Wheeler-DeWitt equation in the minisuperspace for the wave function of universe [69]

$$\frac{d^2\psi}{da^2} - V(a)\psi = 0, \quad (46)$$

where for the case of  $k = 1$

$$V(a) = \frac{1}{l_{Pl}^4} \left( a^2 - \frac{a^4}{r_0^2} \right) \quad (47)$$

where  $r_0$  is given by (13). With this equation we can estimate the probability of tunneling event describing the quantum growth of an initial bubble on its way to the classically permitted region  $a \geq r_0$ , which corresponds to the case of a closed universe inside a black hole as in models of Refs [30,33].

Eq. (46) reduces to the Schrödinger equation

$$\frac{\hbar^2}{2m_{Pl}} \frac{d^2\psi}{da^2} - [U(a) - E]\psi = 0 \quad (48)$$

with  $E = 0$  and

$$U(a) = \frac{m_{Pl} c^2}{2l_{Pl}^2} \left( a^2 - \frac{a^4}{r_0^2} \right) \quad (49)$$

This potential is plotted in Fig.15. It has two zeros, at  $a = 0$  and  $a = r_0$ , and two extrema: the minimum at  $a = 0$  and the maximum at  $a = r_0 \sqrt{2}$ .

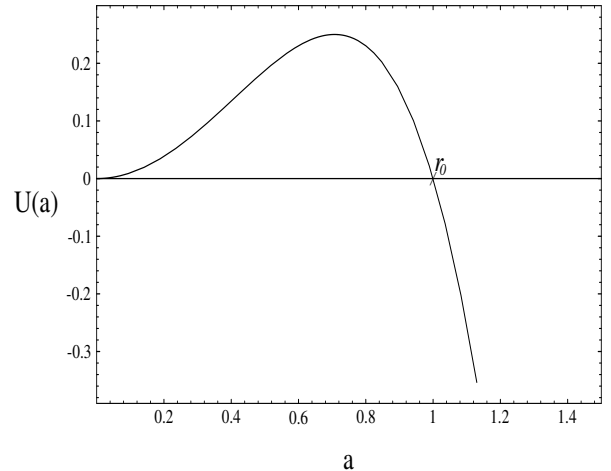


FIG. 15. Plot of the potential Eq.(49).

The WKB coefficient for penetration through the potential barrier reads [47]

$$D = \exp \left( -\frac{2}{\hbar} \left| \int_{a_1}^{a_2} \sqrt{2m_{Pl}[E - U(a)]} da \right| \right) \quad (50)$$

which gives

$$D = \exp \left[ -\frac{2}{3} \left( \frac{r_0}{l_{Pl}} \right)^2 \right] \quad (51)$$

in agreement with the results of Ref. [31].

The probability of a single tunneling event is very small. For the Grand Unification scale  $\sim 10^{15}$  GeV this probability is of order of  $\exp(\frac{2}{3}10^{16})$  (which agrees with the Farhi, Guth and Guven result [31]). However in our case there exists an infinite set of  $\Lambda$ WH structures inside the  $\Lambda$ BH. This strongly magnifies the probability of birth of a baby universe, sooner or later, in one of them.

To estimate probability of quantum birth of an open or flat universe we have to take into account possibility of the equation of state other than  $p = -\rho$  in the initial small seed bubble. We can consider the instability of a  $\Lambda$ WH as evolved from a quantum fluctuation near  $r = 0$ . It is possible to find within this fluctuation, some admixture of quintessence (spatially inhomogeneous component of matter content with negative pressure [13]) with the equation of state  $p = -\rho/3$ . In this case it is possible to find nonzero probability of tunneling for any value of  $k$  [32].

In the Friedmann equation (45) the density evolves with the scale factor  $a$  as

$$\rho = \rho_{vac} \left( \frac{a}{r_0} \right)^{-3(1+\alpha)}, \quad (52)$$

where  $\alpha$  is a factor in the equation of state  $p = \alpha\rho$ . For the de Sitter vacuum  $\alpha = -1$ , and  $\alpha = -1/3$  for the equation of state  $p = -\rho/3$ . When both those components are present in the initial fluctuation, the density can be written in the form [32]

$$\rho = \rho_{vac} \left( B_0 + B_2 \frac{r_0^2}{a^2} \right), \quad (53)$$

where  $B_0$  and  $B_2$  refer to the corresponding contributions.

Then the Friedmann equation (45) takes the form

$$\left( \frac{da}{d\eta} \right)^2 = (B_2 - k)a^2 + \frac{B_0 a^4}{r_0^2} \quad (54)$$

which transforms to the Schrödinger equation (48) with zero energy and with the potential

$$U(a) = \frac{m_{Pl} c^2}{2l_{Pl}^2} \left[ (k - B_2)a^2 - \frac{B_0 a^4}{r_0^2} \right] \quad (55)$$

This potential has two zeros at  $a_1 = 0$  and  $a_2 = \sqrt{(k - B_2)/B_0} r_0$  and two extrema: the minimum at  $a = 0$  and the maximum at  $a = r_0 \sqrt{(k - B_2)/(2B_0)}$ .

The WKB coefficient for penetration through the potential barrier reads now [28]

$$D = \exp \left( -\frac{2}{l_{Pl}} \left| \int_{a_1}^{a_2} \sqrt{(k - B_2)a^2 - \frac{B_0 a^4}{r_0^2}} da \right| \right) \quad (56)$$

The presence of quintessence with the equation of state  $p = -\rho/3$  in the initial fluctuation provides a possibility of quantum birth for the case of both flat ( $k = 0$ ) and open ( $k = -1$ ) universe inside a black hole. The probability of the birth of universe for this case is given by [28]

$$D = \exp \left( -\frac{2}{3} \left( \frac{r_0}{l_{Pl}} \right)^2 \frac{\sqrt{(k - B_2)^3}}{B_0} \right) \quad (57)$$

For  $r_0 \sim 10^{-25}$  cm,  $D = \exp(-\frac{1}{3} \cdot 10^{16})$  for  $k = 0$ ,  $B_0 = 2$ ,  $B_2 = -1$ . This is very close to the value calculated above for the case of  $k = 1$  and  $B_2 = 0$ , and to that obtained by Farhi, Guth and Guven [31]. And, as was pointed above, this small probability of a single tunneling event is magnified in the case of a  $\Lambda$ BH by the infinite number of appropriate  $\Lambda$ WH structures inside of each particular  $\Lambda$ BH.

Let us emphasize, that an obstacle related to the initial singularity, does not arise in general case of distributed profile, since both future and past singularities are replaced by the regular surfaces  $r = 0$ . On the other hand, in the context of creation of a universe in the laboratory, the possibility of influence on the new universe is restricted by the presence of the Cauchy horizon in the de Sitter-Schwarzschild geometry.

### C. Thermodynamics of $\Lambda$ BH

De Sitter-Schwarzschild black hole emits Hawking radiation from both horizons, with the Gibbons-Hawking temperature [34]

$$T = \frac{\hbar \Upsilon}{2\pi k c}, \quad (58)$$

where  $k$  is the Boltzmann constant. The surface gravity  $\Upsilon$  satisfies the equation

$$K_{a;b} K^b = \Upsilon K_a \quad (59)$$

on the horizons, where  $K_a$  is the Killing vector normalized to have unit magnitude at the origin. It is uniquely defined by the conditions that it should be null on both horizons and have unit magnitude at  $r \rightarrow \infty$ . For

de Sitter-Schwarzschild black hole the surface gravity is given by [20]

$$\Upsilon = \frac{c^2}{2} \left[ \frac{R_g(r_h)}{r_h^2} - \frac{R'_g(r_h)}{r_h} \right] \quad (60)$$

with  $r_h$  for both  $r_+$  and  $r_-$ . It has bifurcation point at  $M = M_{crit}$  (extreme black hole) determined by the condition  $g_{00}(r_{\pm}) = g'_{00}(r_{\pm}) = 0$  and given by (27).

For  $\mathcal{M}(r)$  defined by (18) the Hawking temperature is [20]

$$T_h = \frac{\hbar c}{4\pi k r_0} \left[ \frac{r_0}{r_h} - \frac{3r_h}{r_0} \left( 1 - \frac{r_h}{r_g} \right) \right]. \quad (61)$$

Surface gravity characterizes the force that must be exerted at infinity to hold a unit test mass in place at the horizon. It has opposite signs for  $r_+$  and  $r_-$  due to repulsive character of gravity near  $r_-$ . Therefore the temperature on the internal horizon is negative.

The temperature-mass diagram is shown in the Fig.16.

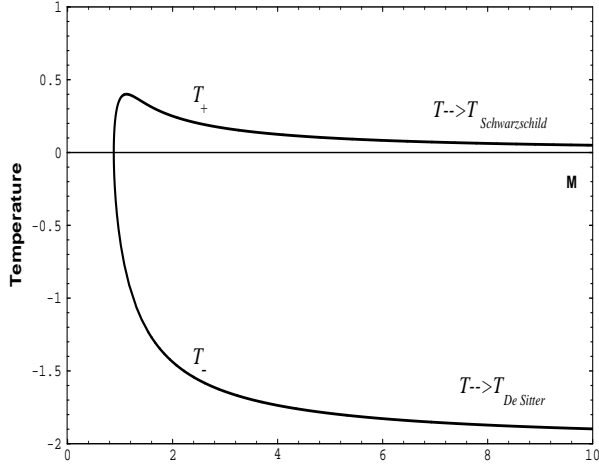


FIG. 16. The temperature-mass diagram for ABH in units  $\hbar = c = G = 8\pi k = 1$ , for the external and internal horizons. The specific heat on the external horizon is positive for  $M_{crit} \leq M \leq M_{tr}$ , where  $M_{crit} \approx 0.3M_{Pl}(\Lambda_{Pl}/\Lambda)^{1/2}$  and  $M_{tr} \approx 0.38M_{Pl}(\Lambda_{Pl}/\Lambda)^{1/2}$ . A second-order phase transition occurs at  $M = M_{tr}$ .

For  $r_g \gg r_0$  the temperature tends to the Schwarzschild value

$$T_{Schw} = \frac{\hbar c^3}{8\pi k G M} \quad (62)$$

on the external horizon and to the de Sitter value

$$T_{deS} = -\frac{\hbar c}{2\pi k r_0} \quad (63)$$

on the inner horizon. Temperature has the maximum at

$$M_{tr} \simeq 0.38M_{Pl}(\Lambda_{Pl}/\Lambda)^{1/2}, \quad (64)$$

and drops to zero when  $r_h$  approaches  $r_+ = r_-$  as  $M$  approaches  $M_{crit}$ . As  $M$  decreases within range of masses  $M_{tr} \geq M \geq M_{crit}$ , the temperature  $T_+$  also decreases. The specific heat is positive in this mass range. In the range of masses  $M > M_{tr}$  temperature grows as black hole loses its mass in the course of Hawking evaporation, approximately according to (62). The specific heat is negative in this mass range. It changes sign as the mass decreases beyond  $M_{tr}$ , hence a second-order phase transition occurs at this point. Temperature of a phase transition is given by

$$T_{tr} \simeq 0.2T_{Pl}(\Lambda_{Pl}/\Lambda)^{1/2} \quad (65)$$

For the case of  $\Lambda \sim \Lambda_{GUT}$  and  $M_{GUT} \sim 10^{15} GeV$ ,

$$T_{tr} \sim 0.2 \times 10^{11} GeV$$

$$M_{tr} \sim 0.4 \times 10^{11} GeV; \quad M_{crit} \sim 0.3 \times 10^{11} GeV$$

Existence of the lower limit for a ABH mass follows in fact from existence of two horizons and does not depend on particular form for the density profile. Temperature drops to zero when horizons merge at a certain value of mass  $M_{crit}$ , and vanishes as  $T \sim M^{-1}$  for  $M \gg M_{crit}$ . It is nonzero and positive for  $M_{crit} < M < \infty$ , since surface gravity is nonzero and positive on the external horizon, in accordance with the laws of black hole thermodynamics. Therefore a curve representing temperature-mass dependence on the external horizon must have a maximum at a certain value of mass  $M_{tr} > M_{crit}$ , which means a second-order phase transition at  $M = M_{tr}$  [20,21].

The vacuum energy outside a ABH horizon is given by

$$E_{vac} = \int_{r_+}^{\infty} \rho(r) r^2 dr = M \exp \left( -\frac{\Lambda}{6GM} r_+^3 \right) \quad (66)$$

One can say that ABH has  $\Lambda$  hair vanishing only asymptotically as  $(r_g/r_0) \rightarrow \infty$ .

In the course of Hawking evaporation, a ABH loses its mass and the configuration evolves towards a AP [20].

#### D. Characteristic surfaces of de Sitter-Schwarzschild geometry

De Sitter-Schwarzschild spacetime has two characteristic surfaces at the characteristic scale  $r \sim (r_0^2 r_g)^{1/3}$ .

The surface of zero gravity is the characteristic surface at which the strong energy condition of singularities theorems [41]  $(T_{\mu\nu} - g_{\mu\nu}T/2)u^\mu u^\nu \geq 0$  (where  $u^\nu$  is any time-like vector) is violated, which means that gravitational acceleration changes sign. The radius of this surface satisfies the condition  $\varepsilon + \sum p_k = 0$ , where  $p_k = -T_k^k$ , and is given by

$$r = r_c = (2r_0^2 r_g/3)^{1/3} \quad (67)$$

The globally regular configuration with the de Sitter core instead of a singularity arises as a result of balance between attractive gravitational force outside and repulsive gravitational force inside of the region bounded by the surface of zero gravity (67).

The surface of zero scalar curvature  $R = 0$  is

$$r = r_s = (4r_0^2 r_g/3)^{1/3} \quad (68)$$

Beyond this surface the scalar curvature changes sign.

Choosing  $r_s$  as the characteristic size of a regular core, we can estimate its gravitational (ADM) mass (18) by

$$m_{core} = 4\pi \int_0^{r_s} \rho r^2 dr \simeq 0.74M \quad (69)$$

Let us note that this mass is confined within the region

$$r_s \simeq 10^{-20} cm (\Lambda_{Pl}/\Lambda)^{1/3} (M/3M_\odot)^{1/3} \quad (70)$$

For a black hole of several solar masses it means that  $\sim 10^{34}g$  is contained in the core of a size  $r_s < 10^{-15} cm$ .

Four characteristic surfaces  $r_+$ ,  $r_-$ ,  $r_c$  and  $r_s$  are plotted in Fig.17.

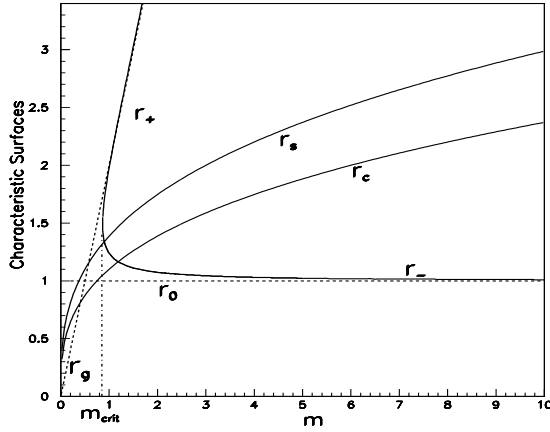


FIG. 17. Surface of zero scalar curvature  $r = r_s$  and of zero gravity  $r = r_c$  (strong energy condition of singularity theorems is violated) are shown together with horizons.

Characteristic surfaces of de Sitter-Schwarzschild geometry exhibit nontrivial behaviour: as mass parameter decreases they change their places before horizons merge, suggesting nontrivial dynamics of evaporation [21]. For nonextreme black hole characteristic surfaces  $r_c$  and  $r_s$  are located between horizons  $r_+$ ,  $r_-$ , in such a sequence that

$$r_- < r_c < r_s < r_+ \quad (71)$$

At the value of mass  $M_c \simeq 0.41M_{Pl}(\Lambda_{Pl}/\Lambda)^{1/2}$ , the surface of zero gravity  $r = r_c$  merges with the internal horizon  $r_-$ , and then for masses  $M < M_c$ , the sequence becomes

$$r_c < r_- < r_s < r_+ \quad (72)$$

At the value of mass  $M_s \simeq 0.31M_{Pl}(\Lambda_{Pl}/\Lambda)^{1/2}$ , the surface of zero scalar curvature  $r = r_s$  merges with the internal horizon, and for masses  $M < M_s$

$$r_c < r_s < r_- < r_+, \quad (73)$$

For the extreme black hole

$$r_c < r_s < r_- = r_+, \quad (74)$$

and for recovered particlelike structure without horizons

$$r_c < r_s \quad (75)$$

In accordance with results of Ref. [52], the de Sitter-like core can approximate the non-Abelian structure with mass  $M = \sqrt{2}gv$ , where  $v$  is the vacuum expectation value of the relevant non-Abelian (Higgs) field with self-interaction  $\lambda = g^2$ . We can estimate a coupling constant  $g$ , setting the Compton wavelength equal to the characteristic size  $r_s$  of a particlelike structure. It results in the formula for the mass  $M = \sqrt{2}gv = M_{Pl}(2\pi\Lambda/\Lambda_{Pl})^{1/4}$ . Taking into account that  $(\Lambda/\Lambda_{Pl}) = (v/M_{Pl})^4$ , we obtain  $g = (\pi/4)^{1/4}$ . Corresponding fine-structure constant  $\alpha = g^2/4\pi$  is  $\alpha = 1/(8\sqrt{\pi}) \approx 1/14$  [20].

## E. Vacuum cores of fundamental particles

De Sitter-Schwarzschild particlelike structure cannot be applied straightforwardly to approximate a structure of a fundamental particle like an electron which is much more complicated. However, we can apply this model to estimate lower limits for sizes of FP, in the frame of our assumption that a mass of a FP is related to its gravitationally induced core with de Sitter vacuum  $\rho_{vac}$  at  $r = 0$ . This allows us to estimate a lower limit on a size of a FP by the size of its vacuum core  $r_c$  defined by the de Sitter-Schwarzschild geometry.

We do this in two cases [23]. First is the case when a lepton gets its mass via the Higgs mechanism at the electroweak scale. Second is the case of maximum possible  $\rho_{vac}$  permitted by causality arguments for a given mass, independently on mechanism of mass generation.

In the context of spontaneous symmetry breaking the false vacuum density  $\rho_{vac}$  is related to the vacuum expectation value  $v$  of a scalar field which gives particle a mass  $m = gv$ , where  $g$  is the relevant coupling to the scalar. For a scalar particle  $g = \sqrt{2\lambda}$  where now  $\lambda$  is its self-coupling. It is neutral and spinless, and we can approximate it by de Sitter-Schwarzschild particlelike structure - in accordance with EYMH results [52]. We identify then the vacuum density  $\rho_{vac}$  of the self-gravitating object with the self-interaction of the Higgs scalar in the standard  $\phi^4$  theory

$$\rho_{vac} = \frac{\lambda v^4}{4} \quad (76)$$

Then the size of a vacuum inner core for a lepton with the mass  $m_l$  is given by

$$r_c = \left( \frac{2m_l}{\pi\lambda v^4} \right)^{1/3} \quad (77)$$

We assume also that the gravitational size of a particle  $r_s$  confining most of its mass, is restricted by its Compton wavelength. This is the natural assumption for two reasons: first, for a quantum object Compton wavelength constraints the region of its localization. Second, it follows from all experimental data concerning limits on sizes of fundamental particles measured by characteristic sizes of interaction regions. For example, for the process  $e^+e^- \rightarrow \gamma\gamma(\gamma)$  at energies around 91 GeV and 130-183 GeV using the data collected with the L3 detector from 1991 to 1997 (for review see [23]) all the sizes of interaction regions are found to be smaller than the Compton wavelength of FP [23].

Applying this constraint for a Higgs scalar we get for its self-coupling  $\lambda \leq \frac{\pi}{16}$ . Vacuum expectation value for the electroweak scale is  $v = 246$  GeV, and an upper limit on a mass of a scalar is given by [23]

$$m_{\text{scalar}} \leq 154 \text{ GeV} \quad (78)$$

The lower limits for sizes of leptons vacuum cores for electron, muon and tau are estimated to [23]

$$r_c^{(e)} > 1.5 \times 10^{-18} \text{ cm}, \quad r_c^{(\mu)} > 0.9 \times 10^{-17} \text{ cm}, \quad (79)$$

$$r_c^{(\tau)} > 2.3 \times 10^{-17} \text{ cm}$$

These numbers are close to experimental constraints. For example, for electron the characteristic size  $R_e$  is restricted by  $e^+e^- \rightarrow \gamma\gamma(\gamma)$  reaction to  $R_e < 1.5 \times 10^{-17} \text{ cm}$ , and the direct contact term measurements for the electroweak interaction constrain the characteristic size for the leptons to  $R_l < 2.8 \times 10^{-18} \text{ cm}$  [23].

To estimate the most stringent limit on  $\rho_{vac}$  we take into account that quantum region of localization given by Compton wavelength must fit within a causally connected region confined by the de Sitter horizon  $r_0$ . This requirement gives the limiting scale for a vacuum density  $\rho_{vac}$  related to a given mass  $m$

$$\rho_{vac} \leq \frac{3}{8\pi} \left( \frac{m}{m_{Pl}} \right)^2 \rho_{Pl} \quad (80)$$

This condition connects a mass  $m$  with the scale for a vacuum density  $\rho_{vac}$  at which this mass could be generated in principle, whichever would be a mechanism for its generation. In the case if FP have inner vacuum mass cores generated at the scale of Eq.(80) (for the electron this scale is of order of  $4 \times 10^7$  GeV), we get the most stringent, model-independent lower limit for a size of a lepton vacuum core

$$r_c > \left( \frac{4}{3} \right)^{1/3} \left( \frac{m_{Pl}}{m_l} \right)^{1/3} l_{Pl} \quad (81)$$

It gives for electron, muon and tau the constraints [23]

$$r_c^{(e)} > 4.9 \times 10^{-26} \text{ cm}, \quad r_c^{(\mu)} > 8.3 \times 10^{-27} \text{ cm}, \quad (82)$$

$$r_c^{(\tau)} > 3.3 \times 10^{-27} \text{ cm}$$

For a scalar of  $\phi^4$  theory produced at the energy scale of Eq.(80), we estimate an upper limit for its vacuum expectation value  $v$  as  $v \leq \sqrt{3m_{Pl}/\pi}$  and get an upper limit for a scalar mass as  $m_{\text{scalar}} \leq \sqrt{3/8}m_{Pl}$ . These numbers give constraints for the case of particle production in the course of phase transitions in the very early universe. In this sense they give the upper limit for relic scalar particles of  $\phi^4$  theory.

Let us emphasize that the most stringent lower limits on FP sizes as defined by de Sitter-Schwarzschild geometry, are much bigger than the Planck length  $l_{Pl}$ , which justifies estimates for gravitational sizes of elementary particles given in the frame of classical general relativity.

#### IV. TWO-LAMBDA GEOMETRY

In the case of non-zero value of cosmological constant at infinity the metric has the form [25]

$$ds^2 = \left( 1 - \frac{R_g(r)}{r} - \frac{\lambda r^2}{3} \right) dt^2 - \left( 1 - \frac{R_g(r)}{r} - \frac{\lambda r^2}{3} \right)^{-1} dr^2$$

$$- r^2 (d\vartheta^2 + \sin^2 \vartheta d\varphi^2), \quad (83)$$

where

$$R_g(r) = r_g \left( 1 - \exp \left( -\frac{\Lambda r^3}{3r_g} \right) \right). \quad (84)$$

The angular components of the stress-energy tensor are given by

$$T_\vartheta^\vartheta = T_\varphi^\varphi = \rho_\Lambda \left( 1 - \frac{\Lambda r^3}{2r_g} \right) \exp \left( -\frac{\Lambda r^3}{3r_g} \right) + \kappa^{-1} \lambda. \quad (85)$$

For  $r \ll (3r_g/\Lambda)^{1/3}$ , the metric (83)-(84) behaves like de Sitter metric with cosmological constant  $\Lambda + \lambda$ , while for  $r \gg (3r_g/\Lambda)^{1/3}$  it achieves the asymptotics of the Kottler-Trefftz solution [44,68]

$$ds^2 = \left( 1 - \frac{r_g}{r} - \frac{\lambda r^2}{3} \right) dt^2 - \left( 1 - \frac{r_g}{r} - \frac{\lambda r^2}{3} \right)^{-1} dr^2$$

$$- r^2 (d\vartheta^2 + \sin^2 \vartheta d\varphi^2), \quad (86)$$

which is frequently referred to in the literature as the Schwarzschild-de Sitter geometry describing cosmological black hole. Our solution (83) represents thus the nonsingular modification of the Kottler-Trefftz solution.



The quadratic invariant of the Riemann curvature tensor  $\mathcal{R}^2 = R_{iklm}R^{iklm}$  is given by

$$\begin{aligned} \mathcal{R}^2 = & 4 \frac{R_g^2(r)}{r^6} + 4 \left( \Lambda e^{-r^3 \Lambda / 3r_g} - \frac{R_g(r)}{r^3} \right)^2 \\ & + \left( \frac{2R_g(r)}{r^3} - \frac{\Lambda^2}{r_g} r^3 e^{-r^3 \Lambda / 3r_g} \right)^2 \\ & + \frac{8\lambda^2}{3} + \frac{16\lambda\Lambda}{3} e^{-\Lambda r^3 / 3r_g} - \frac{4\lambda\Lambda^2}{3r_g} r^3 e^{-r^3 \Lambda / 3r_g} \quad (87) \end{aligned}$$

For  $r \rightarrow \infty$ ,  $\mathcal{R}^2$  tends to the background de Sitter curvature  $\mathcal{R}^2 = 8\lambda^2/3$ . For  $r \rightarrow 0$ ,  $\mathcal{R}^2$  remains finite and tends to the de Sitter value  $\mathcal{R}^2 = 8(\Lambda + \lambda)^2/3$ , which naturally appears to be the limiting value of the space-time curvature. All other invariants of the Riemann curvature tensor are also finite. We see that our solution is regular everywhere.

The two-lambda spacetime has in general three horizons: a cosmological horizon  $r_{++}$ , a black hole event horizon  $r_+$  and a Cauchy horizon  $r_-$ . The metric in general case of three horizons is plotted in Fig.18.

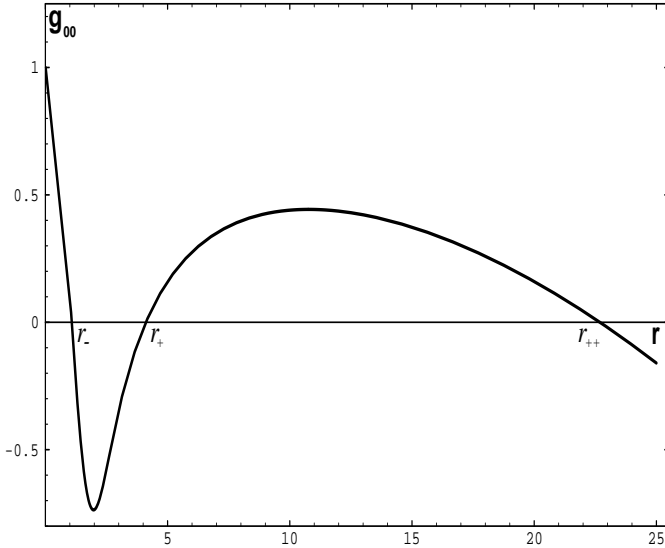


FIG. 18. Two-lambda spherically symmetric solution corresponding to nonsingular cosmological black hole. There are three horizons: an internal horizon  $r_-$ , a black hole horizon  $r_+$ , and a cosmological horizon  $r_{++}$ .

In the region of  $r_h \ll (\Lambda r_g/3)^{1/3}$  we can expand the exponent in the Eq.(84) into the power series. Then we obtain the internal horizon located at

$$\begin{aligned} r_- \simeq & \sqrt{\frac{3}{\Lambda + \lambda}} \left[ 1 + \frac{1}{4r_g} \sqrt{\frac{3}{\Lambda + \lambda}} \left( \frac{\Lambda}{\Lambda + \lambda} \right)^2 \right. \\ & \left. \left[ 1 + \frac{5}{4r_g} \sqrt{\frac{3}{\Lambda + \lambda}} \left( \frac{\Lambda}{\Lambda + \lambda} \right)^2 \right] \right] \quad (88) \end{aligned}$$

for  $r_g \gg \sqrt{3/\Lambda + \lambda}(\Lambda/\Lambda + \lambda)^2$ .

In the region of  $r_h \gg (\Lambda r_g/3)^{1/3}$ , we can neglect the exponential term in Eq.(84) and find the cosmological horizon located at

$$r_{++} \simeq \sqrt{\frac{3}{\lambda}} - \frac{r_g}{2} \quad (89)$$

for  $r_g \ll \sqrt{3/\lambda}(\Lambda/\lambda)$ .

In the interface we are looking for a horizon in the form  $r_h = r_g + \varepsilon$ ,  $\varepsilon \ll r_g$ . That way we get the black hole horizon

$$r_+ \simeq r_g \left[ 1 + \frac{\lambda r_g^2}{3} - \exp\left(-\frac{\Lambda r_g^2}{3}\right) \right] \quad (90)$$

for  $r_g$  within the range  $\sqrt{3/\Lambda} \ll r_g \ll \sqrt{3/\lambda}$ .

In general case the family of horizons can be found numerically. Two-lambda spherically symmetric space-time has three scales of length  $r_g$ ,  $r_\Lambda = \sqrt{3/\Lambda}$ , and  $r_\lambda = \sqrt{3/\lambda}$ . Normalizing to  $r_\Lambda$ , we have two dimensionless parameters:  $M$  (mass normalized to  $G^{-1}\sqrt{3/\Lambda}$ ) and  $q = \sqrt{\Lambda/\lambda}$ . Horizons are calculated by solving the equation  $g_{00}(r) = 0$ . Horizon-mass diagram is plotted in Fig.19 for the case of the density profile given by (25).

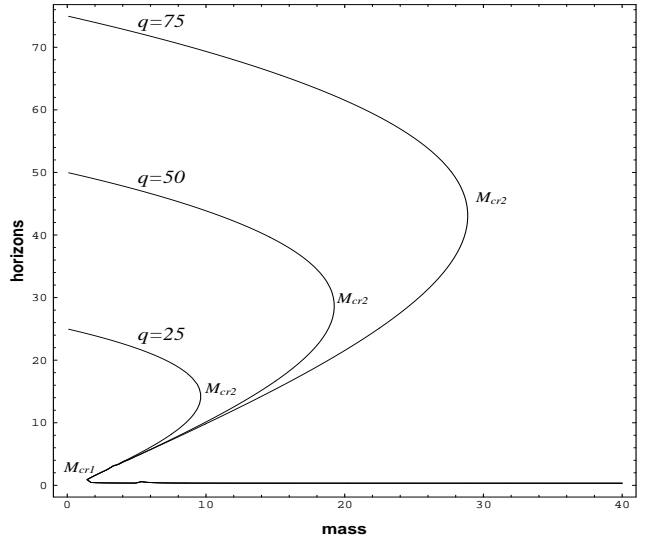


FIG. 19. Horizon-mass diagram for a two-lambda space-time. An upper limit for a BH mass  $M_{cr2}$  depends on the parameter  $q = (\Lambda/\lambda)^{1/2}$ .

Three horizons exist at the range of mass parameter  $M_{cr1} < M < M_{cr2}$ . It follows that there exist two critical values of the mass  $M$ , restricting the mass of a nonsingular cosmological black hole from below and from above. A lower limit  $M_{cr1}$  corresponds to the first extreme BH state  $r_+ = r_-$  and is very close to the lower limit  $M_{crit}$  for  $\Lambda$ BH given by (27). An upper limit  $M_{cr2}$  corresponds to the second extreme state  $r_+ = r_{++}$  and depends on

the parameter  $q \equiv \sqrt{\Lambda/\lambda}$ . Depending on the mass  $M$ , two-lambda geometry represent five types of globally regular spherically symmetric configurations [26]. They are plotted in Fig.20 for the case of the parameter  $q$  defining the relation of limiting values of cosmological constant at the origin and at infinity is given by  $q \equiv \sqrt{\Lambda/\lambda} = 10$ .

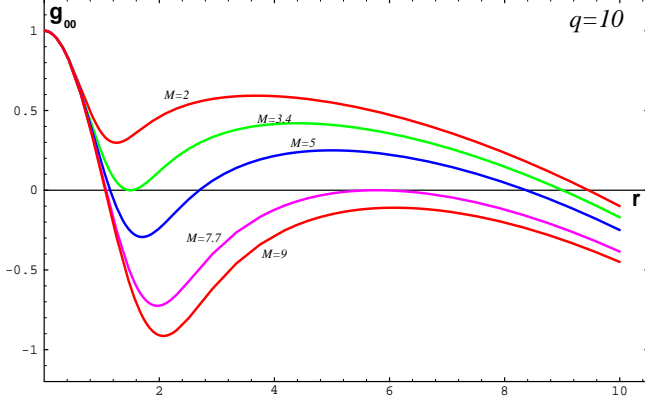


FIG. 20. Two-lambda configurations for the case  $q = 10$ . The mass  $M$  is normalized to  $(3/G^2\Lambda)^{1/2}$ . Two extreme states for  $\Lambda\lambda\text{BH}$  are  $M_{cr1} \simeq 3.4$  and  $M_{cr2} \simeq 7.7$ .

Let us now specify five types of spherically symmetric configurations described by two-lambda solution [25,26].

**Two-lambda black hole** - Within the range of masses  $M_{cr1} < M < M_{cr2}$ , the metric (83) describes a nonsingular nondegenerate cosmological black hole. Global structure of spherically symmetric space-time with three horizons is shown in Fig.21.

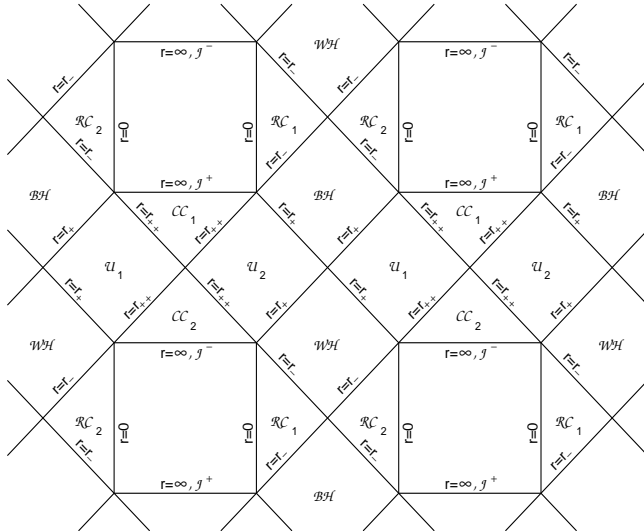


FIG. 21. Penrose-Carter diagram for  $\Lambda\lambda$  black holes. There is an infinite sequence of black and white holes  $\mathcal{BH}, \mathcal{WH}$ , whose singularities are replaced by future and past regular cores  $\mathcal{RC}_1, \mathcal{RC}_2$ , asymptotically de Sitter universes  $\mathcal{U}_1, \mathcal{U}_2$ , and  $\lambda$  cores  $\mathcal{CC}_1, \mathcal{CC}_2$  (regions beyond the cosmological horizons  $r_{++}$ ) and spacelike infinities.

This diagram is similar to the case of Reissner-Nordstrom-de Sitter geometry [12]. The essential difference is that the timelike surface  $r = 0$  is regular in our case. The global structure of space-time contains an infinite sequence of asymptotically de Sitter (small background  $\lambda$ ) universes  $\mathcal{U}_1, \mathcal{U}_2$ , black and white holes  $\mathcal{BH}, \mathcal{WH}$  whose singularities are replaced with future and past regular cores  $\mathcal{RC}_1, \mathcal{RC}_2$  (with  $\Lambda + \lambda$  at  $r \rightarrow 0$ ), and "cosmological cores"  $\mathcal{CC}$  (regions between cosmological horizons and spacelike infinities). Rectangular regions confined by the surfaces  $r = 0$  and  $r = \infty$  do not belong to the diagram.

To specify these regions, we introduce the invariant quantity [55,5]

$$\Delta = g^{\mu\nu} r_{,\mu} r_{,\nu}.$$

Dependently on the sign of  $\Delta$ , space-time is divided into  $R$  and  $T$  regions (see [55,5]): In the  $R$  regions the normal vector to the surface  $r = \text{const}$ ,  $N_\mu = r_{,\mu}$  is spacelike. Therefore in the  $R$  region an observer on the surface  $r = \text{const}$  can send two radial signals: one directed inside and the other outside of this surface. In the  $T$  regions the normal vector  $N_\mu$  is timelike. The surface  $r = \text{const}$  is spacelike, and both signals propagate on the same side of this surface. In the  $T$  regions any observer can cross the surface  $r = \text{const}$  only once and only in the same direction. The  $R$  and  $T$  regions are separated by horizons, where  $\Delta = 0$ . For the space-time considered here,  $\Delta < 0$  in the regions  $\mathcal{RC}$  and  $\mathcal{U}$ , and they are  $R$  regions.  $\Delta > 0$  in the regions  $\mathcal{BH}, \mathcal{WH}$  and  $\mathcal{CC}$ , and those are  $T$  regions. For the metric in the Kruskal form  $\Delta = (1/2)g_{00}^{-1}r_{,u}r_{,v}$  [5]. Since in the  $T$  regions  $\Delta > 0$ , the vector  $r_{,u}$  cannot be zero, and the conditions  $r_{,u} > 0$  and  $r_{,u} < 0$  are invariant. When  $r_{,u} < 0$ , we have  $T_-$  region or the region of contraction (a black hole). When  $r_{,u} > 0$ , we have an expanding  $T_+$  region (a white hole). Near horizons the sign of  $T$  tells us that the vector  $r_{,u}$  enters or goes out of the  $R$  region.

**The lower mass extreme state** - The critical value of mass  $M_{cr1}$ , at which the internal horizon  $r_-$  coincides with the black hole horizon  $r_+$ , corresponds to the first extreme black hole state. For  $M < M_{cr1}$  there is no black hole (see Fig.18), so  $M_{cr1}$  puts the lower limit for a black hole mass. It is given by (27) and practically does not depend on the parameter  $q = \sqrt{\Lambda/\lambda}$ . This extreme black hole is shown in Fig.19 for the dimensionless value of mass  $M = 3.4$ .

Let us compare the situation with the Schwarzschild-de Sitter family of singular black holes. Those black holes have masses between zero and the size of the cosmological horizon (see, e.g., [11]). Replacing a singularity with a cosmological constant  $\Lambda$  results in appearance of the lower limit for a mass of cosmological black hole. It leads thus to the existence of the new type spherically symmetric configuration - the extreme neutral nonsingular

cosmological black hole whose internal horizon coincides with a black hole horizon.

**The upper mass extreme state** - The upper limit  $M_{cr2}$ , at which the black hole horizon  $r_+$  coincides with the cosmological horizon  $r_{++}$ , corresponds to the degenerate black hole existing also in the Schwarzschild-de Sitter family and known as the Nariai solution [54]. What we found here for the case of  $M = M_{cr2}$  is the nonsingular modification of the Nariai solution. As by-product of replacing a singularity by a de Sitter-like core we have in this case additional internal horizon (see Fig.18). The value of  $M_{cr2}$  depends essentially on the parameter  $q = \sqrt{\Lambda/\lambda}$  (see Fig.18). The second extreme black hole is shown in Fig.19 for  $M = 7.7$ .

**Soliton-like configurations** - Beyond the limiting masses  $M_{cr1}$  and  $M_{cr2}$ , there exist two different types of nonsingular spherically symmetric configurations:

(i) In the range of mass parameter  $M < M_{cr1}$  two-lambda solution (83) describes spherically symmetric selfgravitating particlelike structure at the de Sitter background ( $\Lambda_{\mu\nu} \rightarrow \lambda g_{\mu\nu}$  as  $r \rightarrow \infty$ ). This case differs from the case of selfgravitating particlelike structure at the flat space background Fig.2 by existence of the cosmological horizon (see Fig.19 with  $M = 2$ ).

(ii) For  $M > M_{cr2}$  we have quite different type of nonsingular one-horizon spherically symmetric configuration. It differs essentially from the Schwarzschild-de Sitter case by existence of an internal horizon (see Fig.19 with  $M = 9$ ), which comes from replacing a singularity by a de Sitter regular core. It is rather new type of configuration which can be called "de Sitter bag".

## V. SUMMARY AND DISCUSSION

We have presented here the nonsingular modification of the Schwarzschild-de Sitter family of black hole solutions, obtained by replacing a singularity with a de Sitter regular core with  $\Lambda$  at the scale of symmetry restoration. Main features of these geometries:

- 1) algebraic structure of a stress-energy tensor as describing spherically symmetric vacuum corresponding to  $r$ -dependent cosmological term  $\Lambda_{\mu\nu}$
- 2) de Sitter value for spacetime curvature at  $r = 0$
- 3) global structure of space-time,
- 4) existence of the lower limit for a black hole mass,
- 5) second-order phase transition in the course of Hawking evaporation and zero final temperature -

result from the boundary conditions and from the condition  $g_{00} = -g_{11}^{-1}$  imposed for a metric. They do not depend on a particular form of the density profile  $\Lambda_t^t(r)$  if it satisfies condition of finiteness of mass and density.

Global structure of space-time in the case of vacuum nonsingular black holes contains an infinite sequence of

black and white holes whose singularities are replaced with future and past regular cores, at the background of Minkowski or de Sitter space.

A white hole corresponds to nonsingular vacuum-dominated cosmology governed by the time-dependent cosmological term  $\Lambda_{\mu\nu}$  [18]. It models the initial stages of the Universe evolution - nonsingular nonsimultaneous big bang followed by anisotropic Kasner-type stage at which most of a mass is produced [28].

Instability of de Sitter vacuum at the origin can lead to creation of baby universes inside of vacuum black holes. The probability of a single tunneling event is very small, but in our case there exists an infinite number of white hole structures inside each black hole. This highly magnifies the probability of birth of a baby universe via quantum tunneling in one of them.

Replacing a central singularity with a value of a cosmological constant, resulted in appearance of new type of globally regular vacuum-dominated configurations described by the spherically symmetric solutions - vacuum self-gravitating particlelike structures at the background of Minkowski or de Sitter space.

Following Schwarzschild, we can say that "it is always nice to have analytic solution of a simple form". It allows us to investigate behaviour qualitatively and gives a chance to reveal features which otherwise could escape from analysis. For example, numerical analysis of non-Abelian black holes revealed existence, among them, a "neutral" type for which a non-Abelian structure can be approximated as a vacuum core of uniform density [52] (suggesting existence of de Sitter-Schwarzschild black hole), however two essential features of a black hole of this type - existence of the lower limit for a black hole mass  $M_{crit}$  and vanishing the temperature in the course of evaporation - remained concealed. Analytic solution tells us that the form of a temperature-mass diagram is determined by the existence of two horizons. Temperature drops to zero and evaporation stops when the horizons merge in the course of evaporation.

These results allow us to speculate about possible end point for evaporation of a vacuum black hole. One possibility is connected with back-reaction effects. If the back-reaction effects would diminish a mass of the extreme configuration, then a black hole could disappear leaving a cold remnant - a recovered particlelike structure - in its place. We are currently working on investigating its stability. Other possibility is suggested by the global structure of the extreme black hole. In this case the Killing vector  $K$  is not spacelike up to the cosmological horizon, and in principle nothing could prevent internal de Sitter core from exploding. If it would occur, a black hole would evaporate completely. Let us note, that in any case information about baby universes inside a black hole is lost in the course of evaporation.

## Acknowledgement

This talk was supported by the University of Warmia and Mazury in Olsztyn.

- 
- [1] S. L. Adler, Rev. Mod. Phys. **54**, 729 (1982)
  - [2] A. Albrecht and P. J. Steinhardt, Phys. Rev. Lett. **48**, 1220 (1982)
  - [3] N. A. Bahcall, J. P. Ostriker, S. Perlmutter, P. J. Steinhardt, Science **284**, 1481 (1999)
  - [4] V. A. Belinski, E. M. Lifshitz, I. M. Khalatnikov, Sov. Phys. Usp. **13**, 745 (1971)
  - [5] V. A. Berezin, V. A. Kuzmin, I. I. Tkachev, Sov. Phys. JETP **93**, 1159 (1987)
  - [6] B. K. Berger, D. Garfinkle and V. Moncrief, in "Internal structure of black holes and spacetime singularities", Eds. Lior M. Burko and Amos Ori, Inst. Phys. Publ. Bristol and Philadelphia and the Israel Physical Society (1997)
  - [7] M. R. Bernstein, Bull. Amer. Phys. Soc. **16**, 1016 (1984)
  - [8] N. D. Birrell and P. C. W. Davies, "Quantum Fields in Curved Space", Cambridge Univ. Press (1982)
  - [9] H. Bondi, MNRAS **107**, 410 (1947)
  - [10] H. Bondi, T. Gold, MNRAS **108**, 252 (1948)
  - [11] Bouso R. and Hawking S. W., hep-th/970924 (1997)
  - [12] K. A. Bronnikov, Izvestia Vuzov. Fizika **6**, 32 (1979).
  - [13] R. R. Caldwell, R. Dave, P. J. Steinhardt, Phys. Rev. Lett. **80**, 1582 (1998)
  - [14] H. B. G. Casimir, Proc. Kon. Nederl. Akad. **51**, 793 (1948)
  - [15] M.-N. Celerier, J. Schneider, Phys. Lett. **A249**, 37 (1998)
  - [16] B. S. DeWitt, Phys. Rev. **160**, 1113 (1967)
  - [17] A. D. Dolgov, in "The Very Early Universe", p. 449, Ed. G. W. Gibbons, S. W. Hawking, S. T. C. Siclos, Cambridge University Press, England (1983)
  - [18] A. Dobosz, I. G. Dymnikova, in preparation.
  - [19] I. G. Dymnikova, "Nonsingular Spherically Symmetric Black Hole", Preprint Nr 216, Nicolaus Copernicus Astronomical Center (1990); I. Dymnikova, Gen. Rel. Grav. **24**, 235 (1992)
  - [20] I. G. Dymnikova, Int. J. Mod. Phys. **D5**, 529 (1996)
  - [21] I. Dymnikova, in "Internal structure of black holes and spacetime singularities", Eds. Lior M. Burko and Amos Ori, Inst. Phys. Publ. Bristol and Philadelphia and the Israel Physical Society (1997)
  - [22] I. Dymnikova, Gravitation and Cosmology **5**, 15 (1999)
  - [23] I. Dymnikova, A. Hasan, J. Ulbricht, hep-ph/9903526 (1999); I. Dymnikova, A. Hasan, J. Ulbricht, J. Wu, Gravitation and Cosmology **5**, Suppl 230 (1999); I. Dymnikova, A. Hasan, J. Ulbricht, J. Zhao, Gravitation and Cosmology **5**, 1 (2000)
  - [24] I. G. Dymnikova, Phys. Lett. **B472**, 33 (2000)
  - [25] I. Dymnikova, B. Solytsek, in "Proceedings of the VIII Marcel Grossmann Meeting on General Relativity, Ed. Tsvi Piran, World Scientific (1997); Gen. Rel. Grav. **30**, 1775 (1998)
  - [26] I. Dymnikova, B. Solytsek, in "Particles, Fields and Gravitation", Ed. J. Rembielinsky, 460 (1998)
  - [27] I. Dymnikova, A. Magdziarz, B. Solytsek, submitted to General Relativity and Gravitation (2000)
  - [28] I. Dymnikova, A. Dobosz, M. Fil'chenkov, A. Gromov, submitted to Phys. Lett. B (2000)
  - [29] A. S. Eddington, MNRAS **90**, 668 (1930)
  - [30] E. Fahri and A. H. Guth, Phys. Lett. **B183**, 149 (1987)
  - [31] E. Farhi, A. Guth, and J. Guven, Nucl. Phys. **B339**, 417 (1990)
  - [32] M. L. Fil'chenkov, Phys. Lett. **B 354**, 208 (1995)
  - [33] V. P. Frolov, M. A. Markov, and V. F. Mukhanov, Phys. Lett. **B 216**, 272 (1989); Phys. Rev. **D41**, 3831 (1990)
  - [34] G. W. Gibbons and S. W. Hawking, Phys. Rev. **D15**, 2738 (1977)
  - [35] E. B. Gliner, Sov. Phys. JETP **22**, 378 (1966)
  - [36] E. B. Gliner, Sov. Phys. Doklady **15**, 559 (1970).
  - [37] E. B. Gliner, I. G. Dymnikova, Sov. Astr. Lett. **1**, 93 (1975)
  - [38] J. Richard Gott III, Nature **295**, 304 (1982)
  - [39] A. A. Grib, S. G. Mamayev, V. M. Mostepanenko, "Vacuum Quantum Effects in Strong Fields", Friedmann Lab. for Theor. Phys., St.-Petersburg (1994)
  - [40] A. H. Guth, Phys. Rev. **D23**, 347 (1981)
  - [41] S. W. Hawking and G. F. R., "The Large Scale Structure of Space-Time", Cambridge University Press (1973)
  - [42] F. Hoyle, MNRAS **108**, 372 (1948)
  - [43] E. W. Kolb and M. S. Turner, "The Early Universe", Addison-Wesley (1990)
  - [44] F. Kottler, Encykl. Math. Wiss. **22a**, 231 (1922);
  - [45] L. Krauss and M. Turner, astro-ph/9504003 (1995)
  - [46] L.D. Landau and E.M. Lifshitz, Classical Theory of Fields, Pergamon Press (1975)
  - [47] L.D. Landau and E.M. Lifshitz, Quantum Mechanics. Nonrelativistic Theory, Pergamon Press (1975)
  - [48] M.G. Lemaître, C.R. Acad. Sci. Paris **196**, 903 (1933)
  - [49] A. D. Linde, Sov. Phys. Lett. **19**, 183 (1974).
  - [50] A. D. Linde, Phys. Lett. **108B**, 389 (1982)
  - [51] A. D. Linde, "Particle Physics and Inflationary Cosmology", Harwood, Switzerland (1990)
  - [52] Maeda K., Tashizawa T., Torii T., Maki M., Phys. Rev. Lett. **72**, 450 (1994)
  - [53] C. W. Misner, K. S. Thorne, J. A. Wheeler, "Gravitation", Freeman, San Francisco (1973)
  - [54] H. Nariai, Sci. Rep. Tohoku Univ. **35**, 62 (1951)
  - [55] I. D. Novikov and V. P. Frolov, "Physics of Black Holes", Kluwer Academic Publishers (1989)
  - [56] K. Olive, Phys. Rep. **190**, 307 (1990)
  - [57] D.W. Olson, and J. Silk, Ap. J. **233**, 395 (1979)
  - [58] J. P. Ostriker, P. J. Steinhardt, Nature **377**, 600 (1995)
  - [59] J. M. Overduin and F. I. Cooperstock, Phys. Rev. **D58**, 043506 (1998)
  - [60] R. Penrose, in "General Relativity: An Einstein Centenary Survey", Eds. S.W. Hawking and W. Israel, Cambridge Univ. Press, p. 581 (1979)
  - [61] A. Z. Petrov, "Einstein Spaces", Pergamon Press (1969)
  - [62] E. Poisson, W. Israel, Class. Quant. Grav. **5**, L201 (1988)
  - [63] A. D. Sakharov, Sov. Phys. JETP **22**, 241 (1966)
  - [64] W. Shen and S. Zhu, Phys. Lett. **A126**, 229 (1988)
  - [65] M. J. Spornaay, Physica **24**, 751 (1958)
  - [66] A. A. Starobinsky, Phys. Lett. **91B**, 99 (1980)
  - [67] R. C. Tolman, Proc. Nat. Acad. Sci. USA **20**, 169 (1934)

- [68] E. Trefftz, Math. Ann. **86**, 317 (1922)
- [69] A. Vilenkin, Phys. Rev. **D30**, 509 (1984)
- [70] A. Vilenkin, Phys. Rev. **D50**, 2581 (1994)
- [71] S. Weinberg, Rev. Mod. Phys. **61**, 1 (1989)
- [72] Ya. B. Zel'dovich, Sov. Phys. Lett. **6**, 883 (1968)